CONF-9803121--PROC.

UNIVERSITY OF WISCONSIN

CENTER FOR PLASMA THEORY AND COMPUTATION

REPORT

PROCEEDINGS

of the

Workshop on
Nonlinear MHD and Extended MHD

Organizers:
J. D. Callen
University of Wisconsin, Madison, WI 53706-1687
and
W. Park
Princeton Plasma Physics Laboratory, Princeton, NJ 08544

Held at the Radisson Hotel, Atlanta, GA USA

March 25 – 26, 1998

UW-CPTC 98-1

MADISON, WISCONSIN 53706-1687

DISCLAIMER

DISCLAIMER

Portions of this document may be illegible in electronic image products. Images are produced from the best available original document.

WORKSHOP
on
NONLINEAR MHD and EXTENDED-MHD

DATE: March 25 (afternoon) and 26 (full day), 1998

PLACE: Atlanta, Georgia (following the Sherwood Theory Conference)

SCOPE: Numerical and Analytic studies using Nonlinear MHD, and Nonlinear Extended-MHD, such as Kinetic-MHD, Neoclassical-MHD, Psuedo-MHD, Two-fluids, Hybrid Particle/MHD, Fluid/Kinetic, etc, with emphasis on application to experiment

BACKGROUND:

Nonlinear MHD simulations have proven their value in interpreting experimental results over the years. As magnetic fusion experiments reach higher performance regimes, more sophisticated experimental diagnostics coupled with ever expanding computer capabilities have increased both the need for and the feasibility of nonlinear global simulations using models more realistic than regular ideal and resistive MHD. Such extended-MHD nonlinear simulations have already begun to produce useful results. These studies are expected to lead to ever more comprehensive simulation models in the future and to play a vital role in fully understanding fusion plasmas.

This workshop will be in the same spirit as the International one held last April 30 - May 2, 1997 in Madison, Wisconsin, but will be shorter and primarily domestic
in emphasis this year.

TOPICS:

Current state of nonlinear MHD and extended-MHD simulations,
Comparisons to experimental data,
Discussions between experimentalists and theorists,
Equations for extended-MHD models, kinetic-based closures,
Paths toward more comprehensive simulation models, etc.

ORGANIZERS: J.D. Callen (UW)
W. Park (PPPL)

Workshop on
Nonlinear MHD and Extended MHD

March 25 – 26, 1998
Radisson Hotel, Atlanta, GA,

CONTENTS

Brief Overview and Summary

This workshop was a domestic sequel to the international one with the same name [1] held last year in Madison. The ample discussion time provided opportunity for detailed discussion of many modern computational MHD issues among the 25 registered participants. The following paragraphs highlight a few of the key issues discussed. More details are provided in the short written summaries in the remainder of this proceedings.

Problems, Approaches and Codes

The first talk in this session highlighted the current major nonlinear resistive MHD issues in DIII-D (total of 5 with the two simplest, experimentally relevant ones being coupling of resistive and global modes in NCS disruptions, and sawtooth trigger of neoclassical tearing islands). Then, the status of the major extended, nonlinear MHD code projects was reviewed: NIMROD — background, basic code working, being benchmarked on tokamak ideal, resistive MHD instabilities and RFP turbulence simulations; M3D — multi-levels of physics (MHD, two-fluid, gyrokinetic hot particles, gyrokinetic ions), geometry and mesh schemes, simulations being used and benchmarked against experimental reality at each physics level. The ensuing discussion focused on the need for code speedups to facilitate higher level (beyond MHD) physics models and some of the difficulties embodied in using the massively parallel computers, versus the vector spercomputers that are unfortunately being deamphasized.

Simulations

Talks in this session reported on progress in simulating current-drive stabilization of neoclassical tearing modes, use of unstructured meshes to simulate MHD effects of pellet injection, and exploring the comcomitant effects of field line stochasticity and parallel heat conduction during a sawtooth crash. Issues brought out in these talks and the subsequent discussion highlighted the difficulty in equilibrating pressure along magnetic field lines in relevant hot tokamak plasma regimes, and the possible use of 3D curvilinear grids for stellarators and adaptive grids.

Hybrid Models, Simulations

Some of the various approaches and problems in developing fluid/kinetic hybrid simulation models were discussed in this session: development of extended

Chapman-Enskog-like closures for treating parallel heat conduction in low collisionality plasmas, poloidal and toroidal rotation simulations using neoclassical poloidal flow damping closures, simulations with gyrokinetic particle ions and fluid electrons, and drift wave simulations including magnetic perturbation (Alfvèn wave) effects. Most of the discussion in this session emphasized the need to develop models for treating important electron kinetics effects beyond the usual electron fluid models, and proper inclusion of diamagnetic flow and finite ion orbit effects in two-fluid simulations.

Diverse Numerical Approaches

A broader range of simulations was discussed in the final session. These included studies of the instabilities implicated by bifurcated solutions of the ideal MHD equilibrium for stellarators, tearing-mode-induced nonlinear magnetic islands using the "almost ideal MHD" constraint, nonlinear mode coupling damping effects on TAE modes using the CUTIE code, and dramatic demonstrations of the efficiency of using an adaptive mesh algorithm for exploring the dynamics of current sheet formation and magnetic reconnection.

Concluding Discussion

A general feeling at the workshop was that a full simulation of a toroidal plasma discharge with actual physical parameters is not now feasible. Nor is it likely to be so even with computer upgrades and algorithm improvements anticipated over the next 5 years. However, simulations are becoming quite useful in modeling many short-time-scale nonlinear MHD-like phenomena and in developing physical insights. Also, they are on the threshold of being able to quantitatively model most of the important nonlinear MHD-like phenomena in toroidal plasmas, and of being useful for designing efficient experiments to explore these plasma effects and for exploring stabilization techniques near stability boundaries. However, it was also noted that the manpower involved in these developments needs to be expanded by at least a factor of two for this promise to be realized.

Reference

[1] W. Kerner, W. Park, S. Tokuda, J.D. Callen,"Proceedings of the International Workshop on Nonlinear MHD and Extended-MHD," Report UW-CPTC 97-5, April 30 – May 2, 1997.

PROBLEMS IN NONLINEAR RESISTIVE MHD*

A.D. Turnbull, E.J. Strait, R.J. La Haye, M.S. Chu, and R.L. Miller
General Atomics, P.O. Box 85608, San Diego, CA 92138-9784

Linear ideal MHD stability has been remarkably successful in describing many of the general features of DIII–D operation, for example disruption and β limits, resistive wall mode onset, and the general features of the observed modes (whether internal, global, or edge localized for example). Nevertheless, there are several instances where linear ideal magnetohydrodynamics (MHD) does not provide an adequate description of observed phenomena. This is becoming increasingly more common as improved diagnostics provide an unprecedented detailed description of the plasma. The success of ideal MHD in reproducing the general MHD observations gives confidence that the lowest order operation is well understood and that the addition of various nonlinear non-ideal effects to theoretical predictions will greatly expand our predictive capabilities.

A number of research areas and specific problems that are likely to further this goal have been identified. The categories are somewhat arbitrary, but are useful in organizing the individual problems. The list is not intended to be all-inclusive but it does reflect the highest priority topics for DIII–D. These are as follows (not necessarily in priority order).

1. β limit disruptions and β crashes
   a. Nonlinear development of ideal and ideal-like MHD modes near the β limit.
   b. Nonlinear coupling and interaction of multiple MHD modes near the β limit.
   c. Development of overlapping islands into full-scale turbulence and relation to disruptions.
2. Sawtooth physics
   a. Simulation of Kadomtsev and Wesson-type reconnection with observed stability thresholds and fast crash times.
   b. Nonlinear coupling of the $m/n = 1/1$ sawtooth mode with higher n (gongs) and development of seed islands outside $q = 1$.
3. Resistive wall physics
   a. Nonlinear evolution of resistive wall mode and its relation to disruptions and β crashes.
   b. Interaction of resistive wall modes with tearing modes and plasma rotation.
   c. Effect of error fields and mode locking.
4. Neoclassical tearing modes
   a. Nonlinear evolution of neoclassical modes, saturation amplitudes, and role of polarization term.

*Work supported by the U.S. Department of Energy under Grant No. DE-FG03-95ER54309.

5. Fast ion modes
   a. Fast particle stabilization of MHD branch and destabilization of non-MHD fast particle driven modes (fishbones, TAE, BAE, KBM, ...).
   b. Nonlinear development of fast particle driven modes and fast particle expulsion.

Each of these research topics requires specific nonlinear nonideal effects to be included for an adequate description. Table I shows each of the topics with the physics believed to be crucial given by an asterisk (*) and that believed to be useful denoted by a check (✓). The first four rows are clearly necessary in all cases for any realistic success at providing a quantitative comparison with observations. Hence the focus is really on the bottom seven rows. This table can be used in two ways. First, if one assumes a code is given with certain physics elements already modeled, one can use the table to search for appropriate research problems to tackle. We have done this and identified two particular problems that will require minimal additional physics beyond the top four rows for a useful comparison to be made. These are shown highlighted and will be discussed in more detail below.

Alternatively, one can use this table from the point of view of a code developer and look for the physics elements that, if added to a given code, would provide the highest leverage in increasing the applicability of the code to the maximum number of problems. The result of this exercise is clear. Addition of plasma rotation (equilibrium and perturbed) would provide the highest leverage followed closely by the addition of vacuum boundary conditions. This, at least, is the highest priority for DIII–D.

From Table I it is clear that some additional physics beyond the first four rows is necessary in order to treat real problems of experimental interest. Two problems, however, can be identified that could be attacked with only the addition of plasma rotation. These are discussed below.

1. *Nonlinear coupling and interaction of multiple MHD modes near the β limit*

The essence of this problem is the nonlinear coupling between MHD modes that are simultaneously linearly unstable near the β limit. A specific example is of interest here, namely the interaction of localized resistive interchange modes and ideal-like global modes [1] in DIII–D L–mode negative central shear (NCS) discharges near $\beta_N \sim 2$. The latter are believed to be responsible for the observed disruptions. However, the localized resistive interchange modes are also usually present and are likely to play a role also. The localized mode appears often as an early MHD burst at around 50 kHz corresponding to the measured rotation in the core of these discharges where $q' < 0$. The final terminating global mode, however, typically has a lower real frequency around 15 kHz near the measured rotation speed of the minimum in q.

The interaction can be direct or indirect. Indirectly, the localized interchange modes have been found to reduce rotation shear [2] which is known to be destabilizing for the global mode. They also affect the other profiles. In some cases, they appear to be directly coupled as they grow and saturate and slow down until their frequency matches that of the global mode, at which point the global mode rapidly grows and results in disruption [3]. Figure 1 shows the observed frequency spectrum for both types of interaction. Clearly, rotation is crucial for describing the

Table I: Physics required for research problems of direct interest to DIII–D

	β Limit Disruptions			Sawtooth Physics		Resistive Wall			Neoclassical MHD	Fast Ion Effects	
	Nonlinear modes at β limit	Coupling of MHD modes	Overlapping islands turbulence	Reconnection/ sawtooth crash	Coupling 1/1 and $n > 2$	RWM and β crash	RWM and rotation	Error fields/ locking modes	Evolution/ Saturation	MHD versus fast ion branches	Nonlinear fishbones, TAEs, etc.
Toroidal	*	*	*	*	*	*	*	*	*	*	*
Nonlinear	*	*	*	*	*	*	*	*	*	*	*
Finite β	*	*	*	*	*	*	*	*	*	*	*
Resistive	*	*	*	*	*	*	*	*	*	*	*
Rotation	✓	*	*	✓	*	*	*	*	✓	*	*
Vacuum	*	✓	*			*	*	*	✓	✓	*
Resistive wall	✓		✓			*	*	*			
Neoclassical			✓	✓	✓				*		
Two fluid				✓		✓	✓		*	*	*
Multispecies				✓						*	*
Anisotropic p				✓						✓	✓

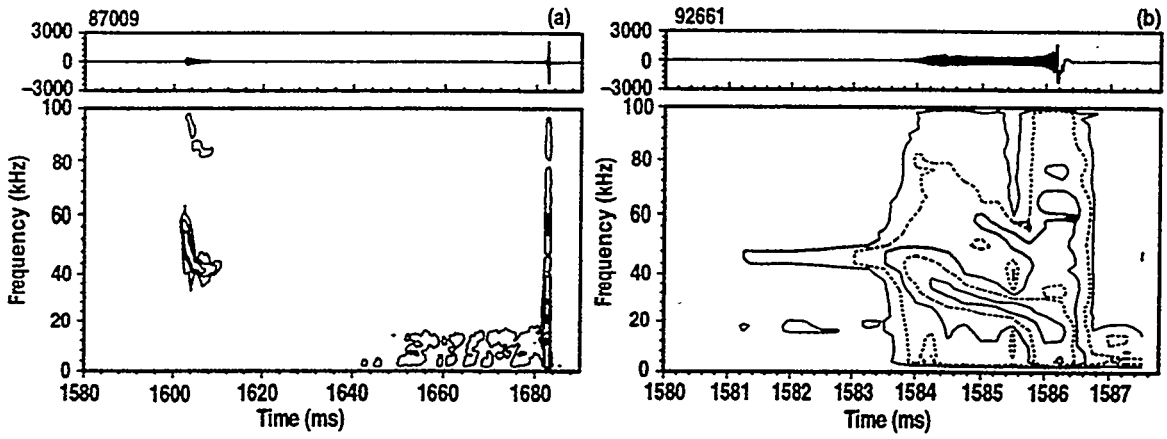

Fig. 1. Coupling between localized resistive interchange mode and global ideal-like mode in L–mode NCS discharges. (a) Indirect coupling: prior localized burst uncoupled but modifies rotation and q profile. (b) Direct coupling: localized mode grows, saturates, and slows to global mode frequency $\Rightarrow$ fast disruption.

interaction. Vacuum boundary conditions would be useful for describing the final disruption but are probably not essential for understanding the essence of the interaction between the modes in the early phase.

2. *Nonlinear coupling of the m/n = 1/1 sawtooth mode with higher n gongs and development of seed islands outside q = 1*

In DIII–D, sawteeth have been observed to trigger $m/n=3/2$ seed islands which subsequently grow and saturate at large amplitude [4]. This subsequent nonlinear evolution is well described by the modified Rutherford equation with neoclassical effects. However, a key unresolved problem is the initial $3/2$ island excitation mechanism and its relation to the sawtooth crash. An example is shown in Fig. 2 which shows the $3/2$ mode appearing on the Mirnov diagnostic immediately after the large sawtooth crash [soft x–ray (SXR) signal] at 2275 ms. Nonlinear mode coupling between the predominantly $m/n=1/1$ kink associated with the sawtooth crash and the $n=2$ mode is clearly essential to model this correctly. The $1/1$ mode is thought to nonlinearly drive an $n/m=2/2$ mode (and probably higher n "gongs") at $q=1$. This should have an $m/n=3/2$ component as well, simply from linear coupling of poloidal harmonics through toroidicity, noncircular cross-section, and finite β. At the crash, the plasma reconnects at $q=1$ but leaves the $3/2$ island. Rotation shear is almost certainly important in modeling this process correctly since it is the most likely cause of the decoupling of the $3/2$ island at $q=1.5$ from the $n/m=2/2$ gong at $q=1$. There may also be a lot of additional effects required to reproduce all the details of the sawtooth crash. However, it does not appear to be essential to correctly model all the details of the crash — the dominant process of interest here is the coupling between different toroidal modes, which should be well described by nonlinear MHD codes.

Data from DIII–D [4] also shows a scaling of the initial $3/2$ island size with magnetic Reynolds number S^{-1}. This scaling is difficult to derive from the neoclassical threshold models

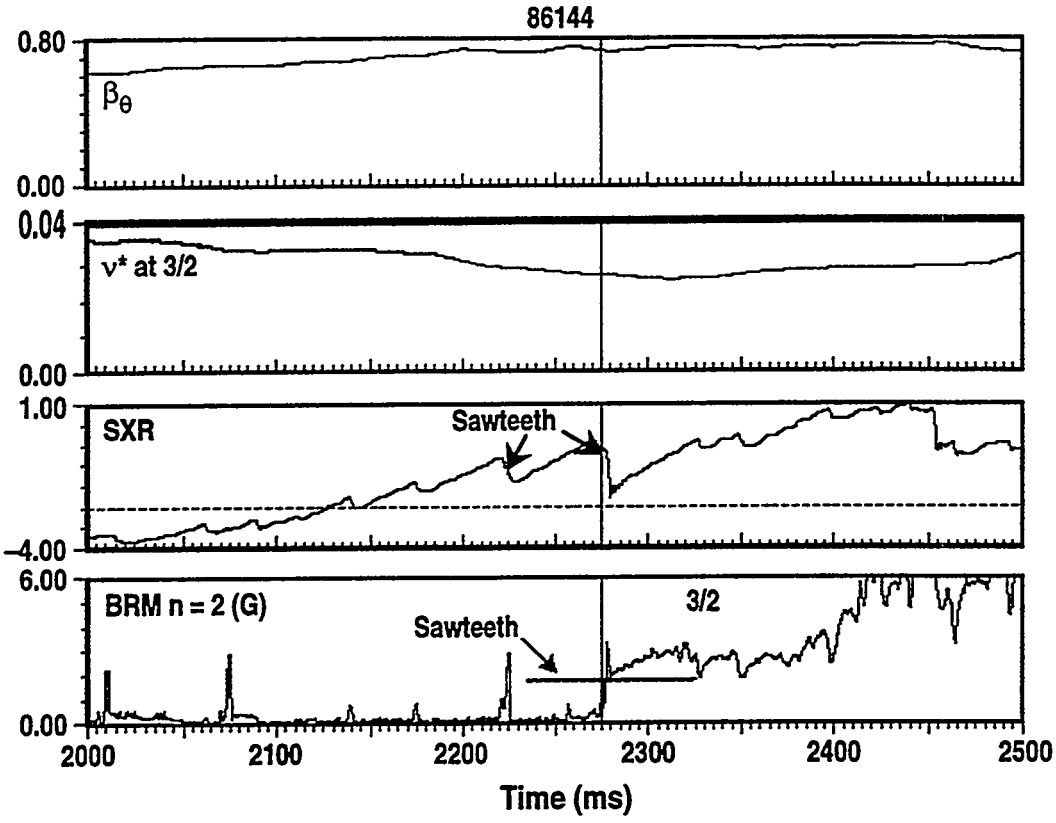

Fig. 2. 3/2 seed island generated by a 1/1 sawtooth crash at 2275 ms.

and, instead, seems to be a consequence of the 3/2 seed island generation. Simulation with a nonlinear MHD code should shed some light on this scaling also.

In conclusion, two experimentally relevant problems can relatively easily be tackled by nonlinear MHD codes. Both problems require plasma rotation in addition to the nonlinear mode coupling and full geometry already incorporated into the codes, but no additional physics seems to be crucial. Addition of plasma rotation to the codes is identified as providing the most leverage for increasing the utility of these codes. Addition of vacuum boundary conditions would also provide high leverage and should be the second highest priority from the point of view of benchmarking the codes against DIII–D.

References

[1] M.S. Chu *et al.*, Phys. Rev. Lett. **77**, 2710 (1996).

[2] L.L. Lao *et al.*, Phys. Plasmas **3**, 1951 (1996).

[3] E.J. Strait *et al.*, Bull. Am. Phys. Soc. **42**, 1845 (1997).

[4] R.J. La Haye and O. Sauter, "Threshold for Metastable Tearing Modes in DIII–D," accepted for publication in Nuclear Fusion.

Nonlinear Simulations with and Computational Issues for NIMROD

Carl R. Sovinec[a] and the NIMROD Team

The NIMROD (Non-Ideal Magnetohydrodynamics with Rotation, Open Discussion) code development project was commissioned by the U. S. Department of Energy in February, 1996 to provide the fusion research community with a computational tool for studying low-frequency behavior in experiments. Specific problems of interest include the neoclassical evolution of magnetic islands and the nonlinear behavior of tearing modes in the presence of rotation and nonideal walls in tokamaks; they also include topics relevant to innovative confinement concepts such as magnetic turbulence. Besides having physics models appropriate for these phenomena, an additional requirement is the ability to perform the computations in realistic geometries.

The volunteers comprising the NIMROD Team are located across the U. S. and Europe, so communication and project organization have challenges that are fitting to the modern age. In fact, a secondary goal of the project is to determine if managerial techniques such as *quality function deployment* and *integrated product development* can help meet these challenges and accelerate the development of a large-scale physics code. There are two notable ways in which these techniques have been applied to the project. First, members of the theory group at General Atomics have represented the interests of customers, and their input and feedback have helped us improve the code in many ways. Second, team meetings at the beginning of the project focused on creating task matrices which link technical goals and customer requirements with properties and features to be developed. This proved very useful for the initial organization of the project, and periodic visitation of the matrices has helped keep the project on track. However, the management techniques did not provide help when unexpected technical difficulties upset the development milestone schedule. Another lesson learned is that having a management expert on the team is important for realizing the potential of these techniques.

Concurrent with the physics kernel development, we have taken several steps to prepare NIMROD for use by people outside the development team. A graphical user interface (GUI) has been developed to facilitate the sequence of preprocessing, code running, and postprocessing. Documentation is being written describing the physics, numerical methods, and programming to make the job of learning NIMROD easier for new users, including those interested in making their own modifications. Finally, the code is portable to many different computer systems ranging from workstations to massively parallel computers to traditional vector supercomputers. Restart files are written in a standard binary format, so that they may be moved from one machine to another.

---

[a] Los Alamos National Laboratory, Los Alamos, NM 87545. e-mail: sovinec@lanl.gov

In its current form, the NIMROD kernel has enough physics to perform nonlinear magnetohydrodynamic (MHD) computations and some two-fluid computations. The equations presently solved are

$$\rho\frac{\partial \mathbf{V}}{\partial t} = \mathbf{J}\times\mathbf{B} - \nabla p + \nabla\cdot\nu\nabla\mathbf{V} - \rho\mathbf{V}\cdot\nabla\mathbf{V}$$

$$\frac{3}{2}\left(\frac{\partial}{\partial t} + \mathbf{V}\cdot\nabla\right)p = -\frac{5}{2}p\nabla\cdot\mathbf{V}$$

$$\mu_0\mathbf{J} = \nabla\times\mathbf{B}$$

$$\frac{\partial \mathbf{B}}{\partial t} = -\nabla\times\mathbf{E}$$

with the generalized Ohm's law including as much as

$$\mathbf{E} = -\mathbf{V}\times\mathbf{B} + \frac{1}{en}\frac{\left(1 - Z_e m_e/m_i\right)}{\left(1 + Z_e m_e/m_i\right)}\left(\mathbf{J}\times\mathbf{B} - \frac{1}{2}\nabla p\right) + \eta\mathbf{J} + \frac{1}{\varepsilon_0\omega_p^2}\left(\frac{\partial \mathbf{J}}{\partial t}\right)$$

plus a linear version of a Hirshman-Sigmar neoclassical closure.[1] At present, there is a single pressure equation, representing the sum of ion and electron pressures, and density is considered constant in time. Eventually, NIMROD will have full two-fluid physics, assuming only quasineutrality and zero displacement current.

Spatial discretization is finite element in the poloidal plane and truncated Fourier series in the toroidal/axial direction—NIMROD can represent either toroidal or periodic linear geometries. The grid is broken into structured blocks of quadrilaterals and unstructured blocks of triangles. This allows us to combine the accuracy and efficiency of a topologically polar grid in the central plasma region with the flexibility of triangular elements near a realistically shaped physical boundary. Dependent variables are treated as bilinear elements within the blocks of rectangles, where equilibrium and geometric quantities are treated as bicubic. In blocks of triangles, all quantities are considered linear.

The solution is advanced from initial conditions with a time-split, semi-implicit algorithm. Though most similar algorithms have the semi-implicit operator for MHD in the velocity advance,[2] in NIMROD it appears in the magnetic field advance in a symmetric but anisotropic form. The linear numerical dispersion relation for this algorithm has no truncation error coupling the shear and compressional Alfven waves,[3] which is important for accuracy when simulating slow resistive MHD behavior with time steps that are large compared to the Alfven time. A separate operator is

also used in the pressure advance. None of the matrices solved each time step couple different Fourier components; coupling only appears in explicit terms that are computed in configuration space after an application of the Fast Fourier Transform.

A predictor/corrector approach is used for each equation containing advection terms. The predictor steps are computed with the semi-implicit operators, as recommended in Ref. 4. We also have the wave-like terms in the predictor steps to avoid effective nonlinear anti-diffusion in the truncation error.[5]

A sample physics application of NIMROD is a simulation of a low aspect ratio reversed-field pinch (RFP), computed in toroidal geometry. Previous numerical RFP studies have been computed in linear geometry. Since the magnetic configuration has safety factor below unity, no linear stabilization is expected from the toroidal geometry, and the approximation is usually appropriate. However, we anticipate that at small aspect ratio, nonlinear coupling is affected. This simulation is the first in a series to explore where the toroidal geometry becomes important and how it manifests itself in the MHD behavior. The simulation has an aspect ratio of 2, the poloidal cross section is circular, the Lundquist number is 1000, and 0-β conditions are assumed. The simulation includes toroidal mode numbers $0 \le n \le 21$. Advection has not been included in the velocity equation in this particular case, and the time step was 0.2 Alfven times throughout the simulation. Figure 1 displays the reversal parameter, $F \equiv \left(\oint dS B_\phi / \oint dS\right)\left(\int dV B_\phi / \int dV\right)^{-1}$, as a function of time. It shows that magnetic field reversal is sustained after the initial saturation at $t=2\times10^{-5}$s. During the last half of the simulation, the magnetic and kinetic energies of the magnetic perturbations are unsteady, which is reflected in the unsteady behavior of the reversed field.

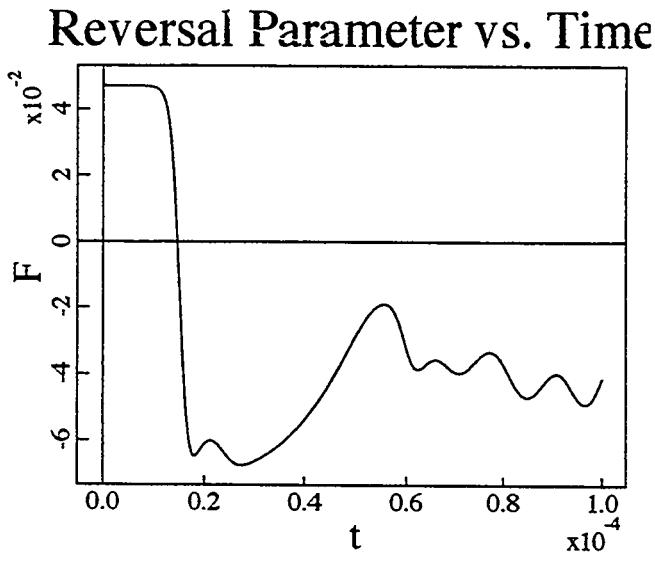

Figure 1. Reversal parameter as a function of time in the toroidal RFP simulation.

With the progress made on the numerical implementation of the plasma fluid equations, validation tests, and new research simulations, the most important issue for the NIMROD project is speed of execution. In most simulations, more than 75% of the CPU time is spent inverting matrices. While the semi-implicit formulation overcomes the stiffness of the Alfven normal modes, the operators in the magnetic field advances lead to ill-conditioned matrices. We have implemented the conjugate gradient scheme with several preconditioning options in the data structures used throughout the code. We are also investigating the possibility of linking the physics kernel to matrix solvers such as AZTEC[6] and ISIS.[7]

Of the computers available to the fusion community, the fastest have massively parallel architectures. We have therefore made the NIMROD kernel a parallel code from the very beginning of its development. When run in parallel, different blocks of the grid are assigned to different processors, and message passing is used to communicate between adjacent blocks. While we have demonstrated favorable scaling on problems run with diagonal preconditioning in the matrix solver, the more powerful preconditioners are sensitive to block decomposition. To reduce the need for grid decomposition, we are presently attempting to assign different Fourier components to different processors. Very little time is spent in the pseudospectral operations, so the components are essentially independent over most of the time step.

To summarize, the NIMROD Team is using contemporary management and computational methods to develop a computational tool for investigating low-frequency behavior in plasma fusion experiments. We intend to make the code freely available, and we are taking steps to make it as easy to learn and use as possible. An example application for NIMROD is the nonlinear toroidal RFP simulation—the first in a series to investigate how toroidal geometry affects MHD activity in RFPs. Finally, the most important issue facing the project at present is execution time, and we are exploring better matrix solvers and a better parallel decomposition to address this.

REFERENCES

[1]S. P. Hirshman and D. J. Sigmar, Nucl. Fusion **9**, 1079 (1981).

[2]for example D. D. Schnack, D. C. Barnes, Z. Mikic, D. S. Harned, and E. J. Caramana, J. Comput. Phys. **70**, 330 (1987).

[3]A. H. Glasser, et al., "Numerical Analysis of the NIMROD Formulation," poster 1C26, 1997 International Sherwood Fusion Theory Conference, Madison, WI.

[4]K. Lerbinger and J. F. Luciani, J. Comput. Phys. **97**, 444 (1991).

[5]R. Lionello, J. A. Linker, and Z. Mikic, "An Improved Semi-implicit MHD Algorithm for PLasmas with Large Flows," Numerical Simulation of Plasmas, Santa Barbara, CA, 1998.

[6]S. A. Hutchinson, J. N. Shadid, and R. S. Tuminaro, "Aztec User's Guide: Version 1.1," Sandia Nat. Lab. Tech. Report SAND95-1559 (October, 1995).

[7]ISIS information is available from http://www.ca.sandia.gov/isis/isis++.html .

M3D Project for Simulation Studies of Plasmas

W. Park, E.V. Belova, G.Y. Fu
Princeton University Plasma Physics Laboratory, Princeton, New Jersey
H.R. Strauss
New York University, New York, New York
L.E. Sugiyama
Massachusetts Institute of Technology, Cambridge, Massachusetts

Abstract
The M3D (Multi-level 3D) project carries out simulation studies of plasmas of various regimes using multi-levels of physics, geometry, and mesh schemes in one code package. This paper and papers by Strauss, Sugiyama, and Belova in this workshop describe the project, and present examples of current applications. The currently available physics models of the M3D project are MHD, two-fluids, gyrokinetic hot particle/MHD hybrid, and gyrokinetic particle ion/two-fluid hybrid models. The code can be run with both structured and unstructured meshes.

1. Introduction

The M3D (Multi-level 3D) project[1] carries out simulation studies of plasmas of various regimes using multiple levels of physics, geometry, and mesh schemes in one code package. More physics levels are also being added for a more complete object oriented code package, which can be used to simulate a wide range of plasma regimes, spanning various fusion devices, space plasmas, and astrophysical plasmas.

Such a general code package would have a profound impact on the search for better confinement schemes. The capability of the code package to apply to a full range of general plasma states will stimulate one's imagination, at the same time requiring it to be firmly based on reality. The interrelations between fusion, space, and astrophysical plasmas borne out by using the same code package would also be of mutual benefit. The object oriented modular code design ensures that carrying the multi-level capability in one code package would incur only a minimal overhead.

The code is currently used to study existing fusion devices. For this application, the benefits include: the most suitable physics, geometry, and grid models, can be chosen for the problem at hand; and running the same problem with physics models of differing complexity aids in physics understanding by isolating the most important physics, and also helps code validation.

The physics levels which are already available and have been used extensively include MHD[2], Two-fluids[4], the hybrid Gyrokinetic Hot Particle/MHD levels.[5–7] Recently, a bulk Ion Gyrokinetic Particle/Two-fluid hybrid level[8] has been added. A Full-kinetic Ion Particle/Fluid Electron hybrid level will be added shortly. For mesh schemes, both structured and

unstructured mesh[9, 10] options are available. Recently, neoclassical parallel viscosity has also been incorporated in the two-fluid level.

In the next sections, physics models and the general structure of the code package are described. Further description of each level and results of current applications are given in papers by Strauss(unstructured mesh MH3D++), Sugiyama(two-fluid MH3D-T), and Belova(bulk ion Gyrokinetic Particle/Two-fluid hybrid level) at this workshop.

2. Physics models

Nonlinear simulation of plasmas is one of the most challenging tasks among computational studies of physical phenomena. Plasma behavior contains many oscillations of vastly different time scales and length scales. Including all these disparate physics in a global simulation, e.g., of a large tokamak will remain difficult at least in the near future. Moreover, even if one could include all the physics in the simulation, the simulation results will be very complex, and it will be difficult to analyze and to acertain its validity.

Our approach is to build a multi-level of physics models, simple to more complete, in the code so that results from levels of differing complexity can be compared to gain physics understanding. This also facilitates a step by step path to a more and more comprehensive simulation code both in development and benchmarking. A physics model of plasmas can be a (configuration space) fluid model which is the moment equations of the kinetic equation, a phase space fluid model such as the Vlasov fluid, a discreet particle model, or a hybrid scheme of the previous three. In general, a fluid model is more efficient computationally, but the closure question remains when collisions are not dominant, which is usually the case in most applications. A phase space fluid model can include all the correct physics, but is computationally very intensive due to the six or five(gyrokinetic) dimensions required. The particle model is the most natural to include all the correct physics with correct boundary conditions, but a very large number of particles is usually required for a reasonable noise level. The δf method[11] for particle simulation is helpful in this regard and is incorporated in the code.

The lower physics levels of M3D are fluid models, and the upper levels consist of particle/fluid hybrid models, because in the medium term, electrons will have to be treated as a fluid. (A particle or a phase space fluid electron model would be too computationally intensive for the medium term, although in a long term these should be also included.) The fluid models give simpler and approximate pictures, while the hybrid models give more complex and accurate ion physics although more computationally intensive. Electron physics will likely remain approximate in the medium term, because no reasonable nonlinear Landau closure scheme exists at present.

The lowest physics level in M3D is the single fluid MHD model which uses the collisional closure and contains the MHD waves(Alfven, fast and slow magnetosonic). The next level is a two-fluid model[4] where the gyroviscous and the neoclassical closures[12, 13] are approximations, e.g., in a banana regime of tokamaks. (We plan to have more accurate neoclassical effects by using separate equations for $P_{\parallel}$ and $P_{\perp}$ with a collision term for both ions and electrons.) The additional effects contained in this level are drift wave, whistler wave, neoclassical effects, mirror modes, etc. The next hybrid Gyrokinetic Hot Particle/MHD level[5, 6] uses gyrokinetic hot particle pressure to couple to the MHD equations, and contains the correct nonlinear hot

particle interactions with waves. and can be used to study nonlinear saturation of TAE, EPM and fishbone modes. The next bulk Ion Gyrokinetic Particle/Two-fluid hybrid level[8] uses the diagonal pressure tensor obtained from gyrokinetic ion particles, and include the bulk ion wave-particle interaction and the ion part of the bootstrap current accurately(when collision is included). The gyroviscosity term is still calculated using a fluid closure. The next physics level planned to be added is the Full-kinetic Ion Particle/Fluid Electron hybrid level, and will be used where $\omega_{ci} \sim \omega_A$ such as in FRC.

The recent applications of the code include high-β disruption[2], off-axis sawteeth[3], pellet injection using an unstructured mesh[9, 10], plasma and island rotation[4], nonlinear saturation of TAE modes[6], and thermal ion particle effects on internal kink[8].

3. Structure of the code package

M3D is designed as much as possible using an object oriented modular code design. The shell is C++ which is an object oriented language, and the core Fortran77 which is more efficient in execution. F90 may be also used in the future. For any large code which is used for cutting edge applications, an object oriented design would be necessary, because what ultimately determines the success of the code in a long run would be how easy it can incorporate newly devised improvements, whether it be a physics model, a mesh scheme, or a numerical algorithm. A modular design (whether object oriented or not) is also necessary for a code with complex multi-level structures to minimize the overhead for carrying the flexible structure. M3D has multi-level structures not only in physics levels, but also in geometry, mesh schemes, boundary conditions, numerical schemes, etc., so that as much as possible modular design is highly desirable. A complete encapsulation of a given module may not be possible at occasion, but efforts should be made to encapsulate as much as possible.

One such example is how we added the unstructured mesh MHD level MH3D++[9, 10] from the structured Fourier space MHD level MH3D. Low level routines which perform differential operations and solution of PDEs such as Poisson's equation are encapsulated in C++ objects to isolate the finite element operations from higher level routines. In this way, the code can be run either in unstructured or in structured mesh, which still holds advantages for some specific problems.

Most of the M3D code is not changed by the use of a different discretization. This allows direct benchmarking of the finite element unstructured mesh level of the code against the original finite difference structured mesh level. The benchmarking tests show that the different levels converge to the same results. The discretization package is in further development to make an array of mesh objects, each with a different boundary shape, with a real space toroidal representation. This is straightforward using the C++ objects, and will allow stellarator simulations with a 3D grid.

4. Conclusion

The M3D (Multi-level 3D) project carries out simulation studies of plasmas of various regimes using multi-levels of physics, geometry, and mesh schemes in one code package. The currently

available physics models of the M3D project are MHD, two-fluids, gyrokinetic hot particle/MHD hybrid, and gyrokinetic particle ion/two-fluid hybrid models. The code can be run with both structured and unstructured meshes. A Full-kinetic Ion Particle/Fluid Electron hybrid level will be added shortly.

Finally, we summarize the basic strategy of M3D project.

- Set a long term goal, but each stage of the development useful by itself.
- Object oriented modular code design: shell in C++, and core in Fortran77 and F90.
- Multi-levels of physics, mesh schemes, boundary conditions, etc., enabling the code for general applications to various laboratory, space, and astro plasmas, for mutual benefit of these fields. For fusion, the multi-level structure allows the testing of any confinement schemes, thereby encouraging invention of better schemes.
- For the medium term, stay within the framework of particle-ion and fluid-electron hybrid models. Particle electrons would be still difficult for most problems.

Acknowledgements

This work was supported by the United States Department of Energy under Contract DE-AC02-76-CHO-3073, Contract DE-FG02-91ER54109, and Grant DE-FG02-86ER53223.

References

[1] W. Park et al., *Plasma Physics and Controlled Nuclear Fusion Research* (IAEA, Vienna, 1997), Vol. 2, p.411.

[2] W. Park et al., Phys. Rev. Lett. **75** 1763 (1995).

[3] Z. Chang et al., *Phys. Rev. Lett.* **77** 3553 (1996)

[4] L.E. Sugiyama et al., This workshop (1998).

[5] W. Park et al., Phys. Fluids B **4**, 2033 (1992).

[6] G. Y. Fu and W. Park, Phys. Rev. Lett. **74** 1594 (1995).

[7] G. Y. Fu et al., *Plasma Physics and Controlled Nuclear Fusion Research* (IAEA, Vienna, 1997), Vol. 2, p.453.

[8] E.V. Belova et al., This workshop (1998).

[9] H.R. Strauss and W. Park, (submitted to Phys. Plasmas, 1998)

[10] H.R. Strauss et al., This workshop (1998).

[11] S. Parker and W.W. Lee, Phys. Fluids B **5**, 77 (1993).

[12] S.P. Hirschman and D.J. Sigmar, Nucl.Fusion **9**, 1079 (1981).

[13] J.D. Callen et al.,*Plasma Physics and Controlled Nuclear Fusion Research* (IAEA, Vienna, 1987), Vol. I, p.157.

Feedback Stabilization of Resistive and Neoclassical Magnetohydrodynamic Tearing Modes in Tokamaks

T.A. Gianakon, X. Garbet, G. Giruzzi, M. Zabiego
CEA Cadarache
France

(March 20, 1998)

Neoclassical tearing modes [1–4] (NTM's) have been projected to be problematic in terms of reduced β limits for fusion reactor concepts that have signficicant bootstrap currents, e.g., ITER. The modes are characterized by a nonlinear threshold for excitation, slow growth rates, and saturation at modest values of the minor radius. The reduction in β is the direct result of quasilinear flattening of profiles within the island. This same feature, through the perturbed bootstrap current, is directly responsible for the drive associated with the instability. Auxiliary current drive from RF waves that is localized and appropriately phased at the resonant rational surface has been proposed as one mechanism to stabilize offending tearing modes [5,6]. The effect can be included in a standard island evolution equation as a Δ'_{aux}, which in general is a complicated function of island width and current localalization. One such form for the evolution of the island width W is

$$0.82\,\frac{dW}{dt} = \Delta' + \frac{W_{nc}W}{W^2 + W_d^2} + \Delta'_{aux}, \tag{1}$$

where W_{nc} is a coefficient that describes the local bootstrap current and $W_d \propto (\chi_\perp/\chi_{||})^{1/4}$ describes the nonlinear threshold for an NTM due to finite perpendicular and parallel transport.

A deceptively simple addition of an auxiliary current to the Ohm's law can be made to model the physics of such stabilization currents on NTM's, but the evaluation of this current in principal requires the solution to a full time-dependent kinetic expression in three dimensional geometry with an island present. Such simulations are beyond the capabilities of the current generation of computers, so that a more simplified model is required. The simplfying approach discussed in this paper extends *neofar*, a neoclassical reduced MHD code [7,8], to include either a direct specification of the RF current drive term in the Ohm's law or an additional evolution equation for this term.

The computational model implemented in the *neofar* code is based in large part on a reduced MHD variant of its parent code *FAR* [9]. As such, *neofar* is an initial value code that separates variables into equilibrium and fluctuation contributions, where fluctuation terms can produce quasi-linear relaxation of equilibrium terms. *Neofar* Fourier decomposes in the poloidal and toroidal directions $(m\theta + n\zeta)$ and uses central differences in the radial direction. This separation allows the linear portion (e.g., a set of poloidally coupled harmonics with the same toroidal mode number) to be solved implicitly with a block tridiagonal solve and nonlinear terms to be dealt with explicitly. Originally, *neofar* was limited to small time steps and long compute times due to the explicit nature of the dominant nonlinear contributions to the parallel transport. Recently, *neofar* has been extensively modified to treat the pressure equation separately from the MHD solve and also fully implicitly, with the effect that all all Fourier harmonics become coupled. This facilitates parallel diffusivities several orders of magnitude larger than in prior simulations and thereby lower thresholds for NTM simulations.

The equations in neofar [7] are a close derivative of reduced MHD [10,11] but with the inclusion of neoclassical effects [12] and RF currents. As such, the neoclassical reduced MHD model consists of a parallel Ohm's law, a vorticity evolution equation, and a pressure evolution equation. The equations are presented elsewhere [8] except for details of the pressure equation and the auxiliary current equation that are presented here.

The first modification to the original equation is that the transport phenomena is assumed to occur on a sufficiently fast time scale relative to the growth of the tearing modes, so that the the full transient pressure equation can be replaced with a diffusive pressure equation that can be solved exactly on each time step, e.g., $\chi_\perp \nabla^2 p_0 = \nabla\cdot(\chi_\perp \nabla p - (\chi_{||} - \chi_\perp)\left[\frac{\vec{B}\vec{B}\cdot\nabla p}{B^2}\right],)$. This assumption lends itself to implementation of a fully implicit solve for the pressure and facilitates values of $\chi_{||}/\chi_\perp \simeq 10^8$ with packed grids near the resonant surface. This value is nominally 100 times larger than the explicit version of neofar, but still represents a value far short of the experimentally relevant values of $\chi_{||}/\chi_\perp \simeq 10^{12}$ [4].

The second modification is the addition of the auxiliary RF current source to the parallel Ohm's law and a new equation for it's solution. The assumption will be made that the RF current source equilibrates on a sufficiently fast time scale so that transients can be ignored. Further, the source term will be described as a diffusive process exactly analagous to the pressure equation, e.g.,

$$\frac{\partial J^\zeta_{RF}}{\partial t} = \chi_\perp \nabla^2 J^\zeta_{RF} + \chi_{||}\vec{B}\cdot\nabla\left(\frac{\vec{B}\cdot\nabla J^\zeta_{RF}}{B^2}\right) + S_{RF} \tag{2}$$

The source term for this auxiliary current equation is dealt with by Fourier expansion to describe the typical scenario of spatial and temporal localization caused by the RF antenna. These set of Fourier coefficients describe a rotating wedge in poloidal and toroidal space. In this case the auxiliary source term can be treated as rotating to overcome difficulties implementing island roation in *neofar*. The souce term is

$$S_{RF} = \sum_{m,n} A_{m,n} \cos(m\theta + n\zeta) + \sum_{m,n} B_{m,n} \sin(m\theta + n\zeta), \tag{3}$$

where the Fourier harmonics are given by

$$A_{m,n} = 2f(\rho)\frac{\sin(m\theta_0)}{\pi\theta_0}\frac{\sin(n\zeta_0)}{\pi\zeta_0}\cos(n\zeta^{on} - n\Omega t)P(t) \tag{4}$$

$$B_{m,n} = 2f(\rho)\frac{\sin(m\theta_0)}{\pi\theta_0}\frac{\sin(n\zeta_0)}{\pi\zeta_0}\sin(n\zeta^{on} - n\Omega t)P(t) \tag{5}$$

$$P(t) = \begin{cases} 1; & \cos(\zeta^{on} - \Omega t) > cos(\zeta^{+}) \\ 0; & \cos(\zeta^{on} - \Omega t) < cos(\zeta^{+}) \end{cases} \tag{6}$$

Here, $f(\rho)$, is the radial localization and is typically taken as a triangle function localized about the resonant surface with width $\Delta\rho$. The source term has a width of $2\theta_0$ in poloidal angle localized on the low-field side about $\theta = 0$ and a width of $2\zeta_0$ in toroidal angle. The auxliary source rotates with frequency Ω and when an appropriate wedge in toroidal angle of width $2\zeta^{+}$ intersects some angle ζ^{on}, the source is turned on, e.g., phasing the current drive. Finally, in the absence of an island, recognition should be made that this diffusive assumption leads to what may be an erroneous result: off axis current drive extends uniformly into the magnetic axis.

For the simulations which follow, a circular cross-section of minor radius $a = 0.80m$, major radius of $R_0 = 2.4m$, toroidal magnetic field of ($I_{wall} = 5.1T$), and central pressure of $\beta_0 = 0.10$ is assumed. The effects of island rotation are neglected by setting $\Omega = 0$. Further, gross simplification of the full toroidal problem is made by neglecting the effects of mode coupling by consideration of only the first 5 resonant harmonics at the q=2/1 surface plus the set of equilibrium harmonics m/n=0/0 through m/n=10/0. The effects of island rotation, RF phasing, and mode coupling are recognized as being extremely important for characterization of the threshold dynamics on real experiments. A radial mesh of 800 grid points is used with variations between a uniform mesh and 3/5 of the grid points localized within 0.05 of the resonant surface. The equilibrium is stable to normal Δ' type tearing modes as evidenced by running the code in the absence of the neoclassical terms. Finally, the bootstrap current is enhanced by a factor of 100 to lower the threshold for the mode. In the absence of this factor of 100 the saturation values are already well in excess of the machine size.

Typical simulation results are presented in Figures 2 and 3 for an NTM resonant at the q=2 surface. In Figure 2, the results are based on an RF current that is simply specified as a single $m/n = 2/1$ harmonic with a trianglar radial deposition factor relative to the resonant surface. In this case, stabilization is readily acheived even down to zero island width with currents approximately 1% of the plasma current at which point the current becomes destabilizing. While this procedure quantatively identifies the amount of current in a particular harmonic that is necessary for stabilization, such a simulation does not address whether such a current perturbation is obtainable in practice. In practice, at island widths on the order of the RF generated current channel, little stabilization is expected, since most of the RF power ends up in the equilibrium harmonic.

In Figure 3, this weakness of direct specification of the current is rectified by considering that the RF depostion must be modified by the island structure, hence the need for Eq. (2). In this case, the RF source term has been optimized for an m/n=2/1 harmonic with parameters of $\delta_r = 0.03$, $\theta_0 = \pi/2$, and $\zeta_0 = \pi/4$. The initial observation is that the currents required for stablization appear to be very large. These values however must be rescaled by a factor of 1/100 to account for the 100 times enhancement of the bootstrap current. Thus for an island with $W \simeq 0.06a$, an RF current of 2 to 3% of the plasma current is required to saturate the mode. An additional factor of 5 is also justified, since the simulation is limited to the case of $W < 0.2W_d$, where $W_d \simeq 0.25a$ for this simulation. Since the largest growth rate for the instabilty occurs at $W = W_d$ at least a factor of 5 increase in the stabilization current is suggested. This would assume that in the real experiment one really begins stabilization after the mode has saturated. The conclustion would then be that the RF current required for stabilization is about 10% of the plasma current.

Several additional observations can be made based on Figure 3 for the case the case when $I_c/I_p = 2.81$. In this case, the mode saturates at a width approximately the same as the current channel width, but then the stabilization is lost. In this case, the stabilization is lost because a significant $m/n = 0/0$ harmonic of the equilibrium current

is generated which modifies the q-profile. The localization of the RF current then shifts away from the appropiate surface, which effectively reduces the amount of current available for stabilization, and has the added effect of putting even more current into the 0/0 harmonic. This effect would probably be lessened if simulations could be conducted at the experimentally relevant range, since then instead of putting 3 times the plasma current at the resonant surface only about 0.1 the plasma current would be introduced.

---

[1] See National Technical Information Service Document No. DE6008946 (W.X. Qu and J.D. Callen, "Nonlinear Growth of a Single Neoclassical MHD Tearing mode in a Tokamak", U.W. Plasma Report 85-5 (1985).) Copies may be ordered from the National Technical Information Service, Springfield, VA 22161

[2] R. Carrera, R.D. Hazeltine, M. Kotschenreuther, Phys. Fluids **29**, 899 (1986).

[3] C.C. Hegna, J.D. Callen, Phys. Fluids **4**, 1855 (1992).

[4] N.N. Gorelenkov, R.V. Budny, Z. Chang, M.V. Gorelenkova, L.E. Zakharov Phys. Plasmas **3**, 3379 (1996).

[5] E. Lazzaro, G. Ramponi, Phys. Plasmas **3**, 978 (1996).

[6] C.C. Hegna, J.D. Callen, Phys. Plasmas **4**, 2940 (1997).

[7] T.A. Gianakon, PhD Thesis (Univeristy of Wisconsin-Madison, 1996) & (T.A. Gianakon, UW-CPTC 96-1).

[8] T.A. Gianakon, C.C. Hegna, J.D. Callen, Phys. Plasmas **5**, 4637 (1996).

[9] L.A. Charlton, J.A. Holmes, H.R. Hicks, V.E. Lynch, B.A. Carreras, J. of Comp. Physcis **63**, 107 (1986) .

[10] H.R. Strauss, Nuclear Fusion **23**, 649 (1983).

[11] R.D. Hazeltine and J.D. Meiss, Phys. Reports **121**,1 (1985).

[12] J.D. Callen, W.X. Qu, K.D. Siebert, B.A. Carreras, K.C. Shaing, D.A. Spong, *in* Plasma Phys. & Cntl Nucl Fus Rsch 1986 (International Atomic Energy Agency, Vienna, 1987), Vol. I, p. 157.

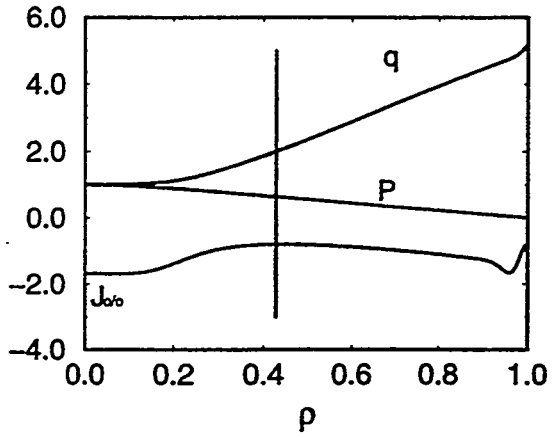

FIG. 1. Equilibrium profiles used in the study of NTM's.

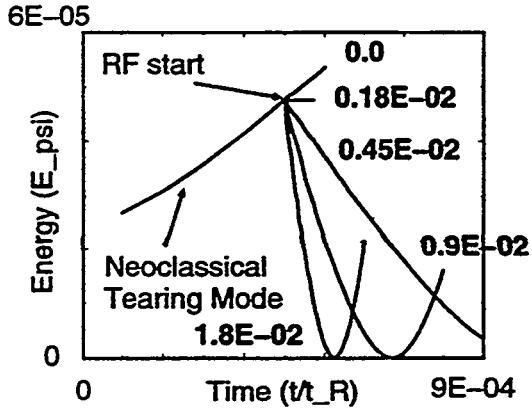

FIG. 2. Power scan of the auxiliary current for stabilization of an NTM by direct specification of this current.

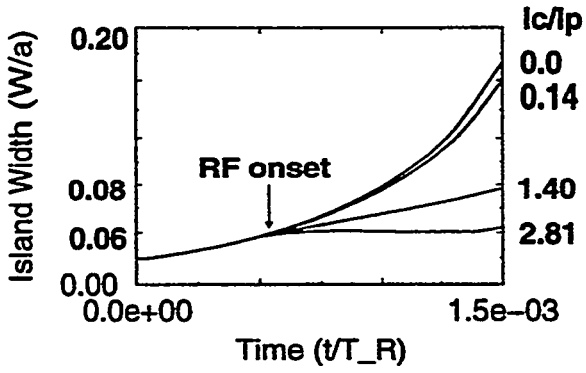

FIG. 3. Power scan of the auxiliary current for stabilization of an NTM by solution of a current evolution equation.

MHD Simulations on an Unstructured Mesh

H.R. Strauss, *NYU*
W. Park, E. Belova, G.Y. Fu, *PPPL*
D. W. Longcope, *University of Montana*
L.E. Sugiyama, *MIT*

Two reasons for using an unstructured computational mesh are adaptivity, and alignment with arbitrarily shaped boundaries. Two codes which use finite element discretization on an unstructured mesh are described. FEM3D solves 2D and 3D RMHD using an adaptive grid. MH3D++, which incorporates methods of FEM3D into the MH3D generalized MHD code, can be used with shaped boundaries, which might be 3D.

Adaptive Mesh MHD

Adaptive methods for MHD have used both unstructured [1, 3] and structured grids [2]. The main computational difficulty with an unstructured, adaptive mesh is the accurate calculation of the current. The most effective solution is to employ a current - vorticity advection formulation of the equations. Acceptable results can also be obtained with a two - step calculation of the current from the vector potential. Mesh operations are described to reconnect and refine the mesh adaptively in the vicinity of nearly singular currents. Example computations of the coalescence instability, tilt mode and divertor tokamak equilibrium, validating and illustrating the method, are presented. The simulations show the formation of current sheets, with the current density increasing exponentially in time. During this increase, the grid of initially $\sim 10^4$ points adapts to provide resolution comparable to a uniform grid of up to 5×10^6 grid points.

The equations can be discretized using piecewise linear, triangular finite elements. Three sparse matrices, the mass matrix, stiffness matrix, and bracket tensor, arise in the discretization. Their construction and assembly is discussed. The stiffness matrix can cause a convergence problem in computing the current, for which we give two possible cures. The most effective cure is to use symmetrized MHD equations, in which vorticity and current are time advanced, and the potentials are found by solving Poisson equations. The other approach is to use a modified stiffness matrix with a wider stencil, having acceptable convergence properties.

Adaptive gridding is done with two mesh operations: splitting pairs of triangles into four triangles; and the inverse operation of combining four triangles into two.

As an example and test of the method, we first consider the periodic coalescence instability [4]. The initial equilibrium Fig.1(a) consists of an array of cells with periodicity is built into the mesh by the connectivity of the mesh triangles.

As the simulation evolves, the current density becomes concentrated into thin sheets located at the short side of the pentagonal separatrix. A blowup of the plot of the current density at time $t = 0.21$ is shown in Fig.1(c). The current is well resolved and unremarkable in structure. A similar blowup of the mesh on which the current is calculated is shown in Fig.1(d). The minimum length scale of the mesh is .022 the length of the original mesh cells, which is equivalent to a mesh of $5,000,000$ mesh points. In fact the mesh has only $10,400$ mesh points.

The peak value of the current density grows exponentially in time, with a large growth rate more than 10 times the linear mode growth rate. Exponential growth is predicted theoretically [5]. As the current density increases, so does the number N of mesh points.

The FEM3D code has also been applied to 3D RMHD, such as the calculation of nonlinear edge localized pressure driven modes in divertor geometry, including a magnetic separatrix in the computational domain [6].

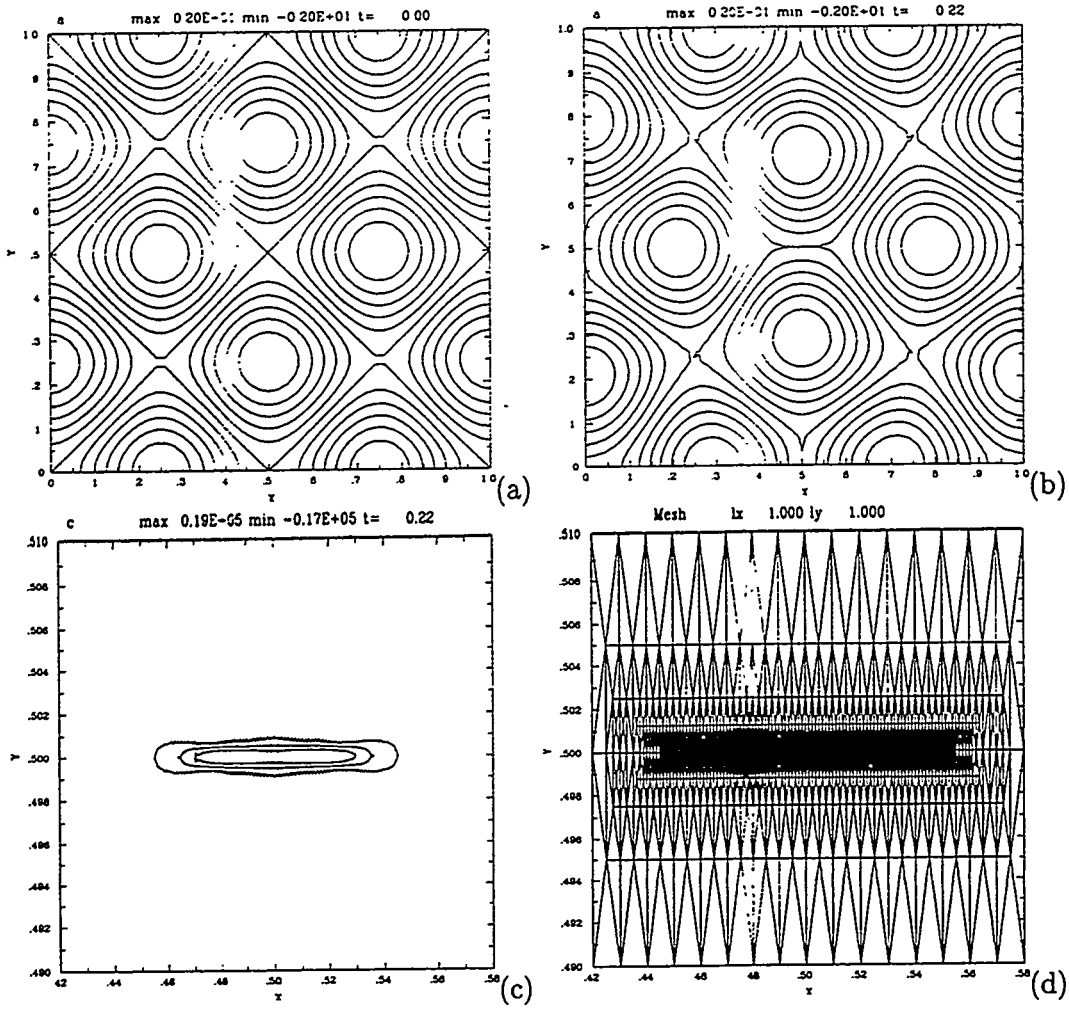

Figure 1: (a) A calculation of the coalescence instability. Contours of magnetic flux ψ at time $t = 0$. (b) Contours of magnetic flux ψ at time $t = 0.21$ (c) A blowup view of contours of current C at time $t = 0.21$ The view is centered on the separatrix, on short side of a flux pentagon. The horizontal scale is about 0.2 of the scale ℓ of the previous figure, while the vertical scale is about 0.04ℓ. (d) A blowup view of the mesh around the the current sheet. The minimum scale length of the mesh is 0.022 the size of the initial mesh separations.

MH3D++ Unstructured Mesh Code

The most efficient way to represent general geometric effects is to use an unstructured numerical mesh. MH3D++ is the unstructured mesh finite element version of the MH3D code [?]. Low level routines which perform differential operations and solution of PDEs such as Poisson's equation are encapsulated in C++ objects to isolate the finite element operations from higher level routines. In this way, the code can be run either in unstructured or in structured mesh versions, which still holds advantages for some specific problems. The results of MH3D++ converge to MH3D results. The MH3D++ code has been given an option of a finite difference discretization in the toroidal direction, replacing the spectral representation. This permits efficient parallelization. The next step is to use an array of mesh objects to build a three dimensional mesh, which will be used for resistive, nonlinear stellarator simulations.

MHD Effects on Pellet Injection

Recent ASDEX results [9] demonstrated that pellets injected on the inboard, low major radius edge, suffered less loss, and were absorbed more completely into the plasma. Efficient pellet penetration is important for very large size, long pulse tokamaks, such as ITER.

Nonlinear MHD simulation results of pellet injection [7] withthe MH3D++ code show that MHD forces can accelerate large pellets, injected on the high field side of a tokamak, to the plasma center, reconnecting the magnetic field into a reverse shear configuration. Ballooning instability caused by pellets is also reduced by high field side injection. Studies are also reported of the current quench phase of disruptions, which can cause 3D halo currents and runaway electrons. A scaling law is obtained for pellet displacement which agrees well with the simulations.

The simulations are initialized with a two dimensional MHD equilibrium, to which a pellet is added. The simulations assume that the pellet ionizes and ablates rapidly, compared to the Alfvén and sound wave time scales. The pellet is the source of a plasma cloud, which has a non uniform density and pressure distribution on magnetic surfaces. The pellet cloud contributes no energy to the plasma; the flux surface averaged pressure profile is the same as without the pellet. The three dimensional perturbed non equilibrium plasma relaxes by parallel streaming of heat and density, and major radius displacement akin to the Shafranov shift. Driven magnetic reconnection imparts some non reversibility to the effect. This is shown particularly in the case of inboard injection, where the pellet cloud penetration changes the q profile to a reverse shear profile.

MHD Disruptions caused by pellet injection

Further studies are being carried out on disruptions initiated by pellets. We start with a high β equilibrium and insert a pellet perturbation. A pellet ablation cloud 3D pressure perturbation can trigger moderate m pressure driven instabilities.

As with pellet injection, there are advantages to the high magnetic field side. Pellets on the inside require a larger pressure perturbation to trigger an instability. The equilibrium pressure gradient adds to the pellet pressure gradient for low field side instability, while the equilibrium pressure gradient subtracts from the pellet pressure gradient for high field side instability. In addition, on the low field side, the velocity perturbations resemble typical moderate wavelength ballooning modes. They produce disruptions in nonlinear simulations. On the high field side, the velocity perturbations are much more localized. They might simply cause the breakup and more rapid dispersion of the pellet cloud.

3D Disruptions, Halo Currents, and Runaways

Another category of work with MH3D++, which is relevant to ITER and other large tokamaks, concerns halo currents and runaways generated during the current quench phase following major disruptions. Halo currents caused by 3D kink modes in the latter phases of a disruption could cause serious mechanical load problems. In addition, runaway electron currents could be channeled to the wall by the 3D magnetic field perturbations, causing wall damage. Disruption simulations are being carried out which have both a self consistent three dimensional resistivity proportional to the temperature to the $-3/2$ power, as well as a thin resistive shell through which the plasma magnetic field is coupled to an external vacuum field. Preliminary results indicate significant 3D peaking factors. Runaway generation by avalanching will be modeled [10].

Summary

Unstructured mesh methods are useful for adaptive MHD simulations, as illustrated by FEM3D. Use of an unstructured mesh has extended the capability of the MH3D extended MHD code to computations involving curvilinear geometry. MH3D++ could be improved by extending the approach to 3D curvilinear grids, for stellarator applications. MH3D++ could be further improved by adding adaptivity, which would be useful for e.g. the pellet problem.

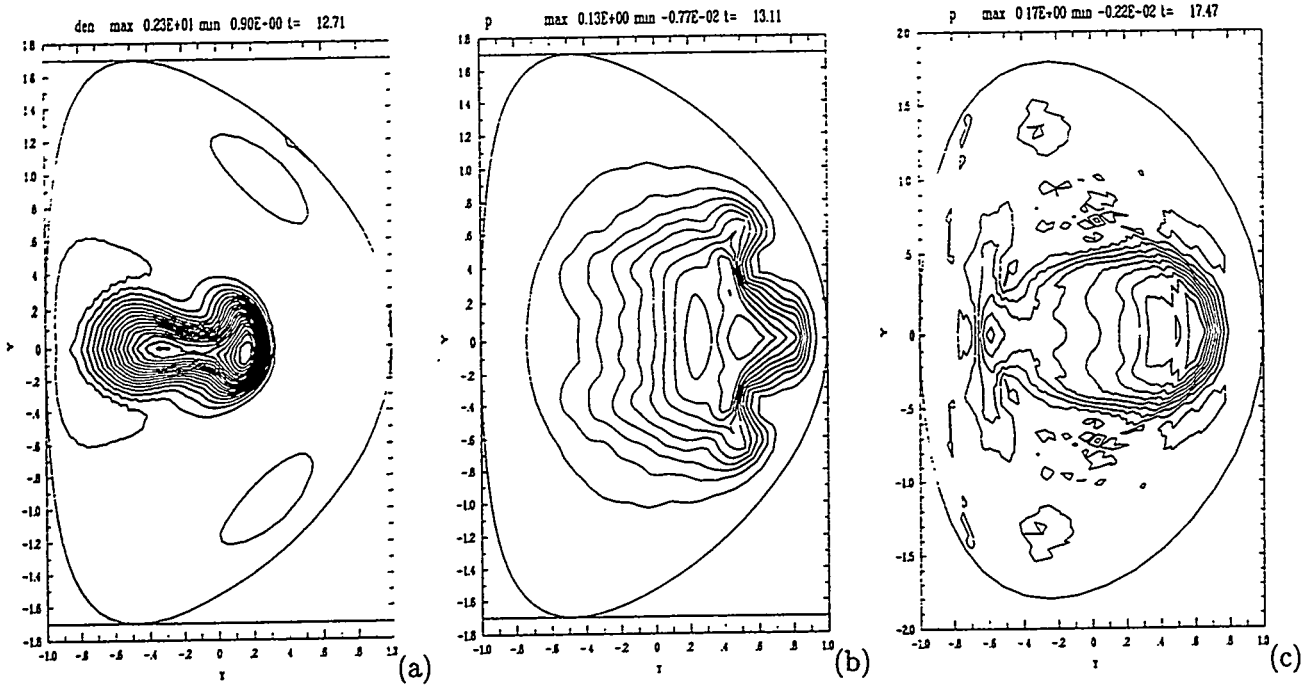

Figure 2: Fig.2(a) shows pellet cloud density contours in the $\phi = 0$ poloidal plane at $t = 12.7R/v_A$. The pellet was inserted on the high field side, and was accelerated by toroidal curvature forces, causing it to move to the magnetic axis. In the process it causes magnetic reconnection to a reverse shear profile. Fig.2(b) shows pressure contours in the $\phi = 0$ poloidal plane at $t = 13.1R/v_A$. In this case a pellet was inserted on the low field side, increasing the local pressure gradient enough to cause an instability. The nonlinear development of the instability is shown. Fig.2(c) shows pressure contours in the $\phi = 0$ poloidal plane at $t = 17.5R/v_A$. This is a kink simulation of the current quench phase of a disruption.

This work was supported by the United States Department of Energy under Grant DE-FG02-86ER53223 and Contract DE-AC02-76-CHO-3073.

References

[1] H. R. Strauss and D. W. Longcope, submitted to J. Comp. Phys., 1998.

[2] H. Friedel, R. Grauer and C. Marliani, J. Comp. Phys. **134**, 190 - 198 (1997).

[3] D. D. Schnack, I. Lottati, Z. Mikić, and P. Satyanarayana, J. Comp. Phys., to appear, 1998.

[4] D. W. Longcope and H. R. Strauss, Ap. J. 426:742-757, (1994).

[5] I. Klapper, Physics of Plasmas, *to appear*, (1998).

[6] H. R. Strauss, Phys. Plasmas *3*, 4095 (1996).

[7] H. R. Strauss and W. Park, Magnetohydrodynamic effects on pellet injection in tokamaks, submitted to Phys. Plasmas (1998).

[8] W. Park, Z. Chang, E. Fredrickson, G. Y. Fu, N. Pomphrey, H. R. Strauss, and L. E. Sugiyama, Sixteenth IAEA Fusion Energy Conference, Montreal, F1-CN-64/D2-2 (1996)

[9] P.T. Lang, K. Buechl, M. Kaufmann, R.S. Lang, *et al.*, Physical Review Letters 79, 1487-1490 (1997)

[10] M. N. Rosenbluth and S. V. Putvinski, Nuclear Fusion *37*, 1355 (1997).

Resolving magnetic field line stochasticity and parallel thermal transport in MHD simulations

Y. Nishimura, J. D. Callen, and C. C. Hegna

Department of Engineering Physics,

University of Wisconsin-Madison, Wisconsin, 53706-1687

Heat transport along braided, or chaotic magnetic field lines is a key to understand the disruptive phase of tokamak operations, both the major disruption and the internal disruption (sawtooth oscillation). Recent sawtooth experimental results in the Tokamak Fusion Test Reactor (TFTR) [1] have inferred that magnetic field line stochasticity in the vicinity of the $q = 1$ inversion radius plays an important role in rapid changes in the magnetic field structures and resultant thermal transport.

In this study, the characteristic Lyapunov exponents and spatial correlation of field line behaviors are calculated to extract the characteristic scale length of the microscopic magnetic field structure (which is important for net radial global transport). These statistical values are used to model the effect of finite thermal transport along magnetic field lines in a physically consistent manner. stimate of the cross field diffusion we postulate a form given by

$$\chi_{eff} = \int_{-\infty}^{\infty} - \quad \rho\left(-\frac{\zeta^2}{4\chi_{||}}\right)\left(\frac{\zeta h}{2\pi R}\right)^2 d\zeta, \tag{1}$$

which includes the c decorrelation effects of fast thermal streaming along the field lines moderated by collisi re ζ is the toroidal angle, $\chi_\perp$ and $\chi_{||}$ stand for perpendicular and parallel heat condu efficient normalized by resistive time scale and the minor radius. Note the value of χ_e ıcrease linearly with $\chi_{||}$.

Numerical simulations have been conducted by using the three dimensional nonlinear initial value MHD code FAR[2]. Parameters used in the calculations shown here are: aspect ratio $\epsilon = 0.25$, Lundquist number $S = 10^5$. The safety factor was taken to be in the range of $0.81 \leq q \leq 2.7$. Toroidal mode numbers were taken up to $1 \leq n \leq 10$ (total of 151 modes). A total of 500 equally spaced mesh points were used in the radial direction.

With higher β simulations, a sudden onset of Alfven time scale pressure driven mode[3] is observed in the final stage of the sawtooth crash. Figures 1 shows pressure contours in a poloidal cross section $\zeta = \pi$ and $\zeta = 0$, in the absence of parallel conduction. Typical ballooning type structure (a finger) on the bad curvature side can be seen starting from $t = 1440t_a$; the $m/n = 1/1$ magnetic island evolution gave rise to convection of the pressure inside the inversion radius and builds up steep pressure gradient across the island separatrix or the Y-ribbon[4], and thereby trigger ballooning instabilities below the threshold at the equilibrium. Also indicated was the strong coupling of the 1/1 mode to the 2/1 and the 0/1 modes, which is indicative of

dispersion of the current free energy inside $q = 1$ surface. In this specific case, a maximum β of 5% was taken.

The resultant pressure evolution in response to the stochastic magnetic field lines has also been investigated. From a simulation above, we found the maximum value of the stochasticity induced thermal diffusion to be $\chi_{eff} \sim 10$ for the $\chi_{||} \sim 10^3$ value employed here. In this work, $\chi_{\perp} = 0.1$ was taken so that the χ_{eff} value described above dominates the pressure response to the stochastic field lines. Figure 2 shows the pressure contour in the presence of finite $\chi_{||}$. The differences with Fig. 1 suggest ergodization of pressure within the stochastic magnetic field line regions. Qualitative investigation of the ballooning mode spectrum will be presented.

This research was supported by United States Department of Energy Grant No. DE-FG02-86ER53218.

References

[1] Y. Nagayama et al., Phys. Plasmas **3**, 2631 (1996); J. D. Callen, B. A. Carreras, and R. D. Stambaugh, Phys. Today **45**, 34 (1992); M. Yamada et al., Phys. Plasmas **1**, 3269 (1994).

[2] L. A. Charlton et al., J. Comput. Phys. **86**, 270 (1990); Y. Nishimura, J. D. Callen, and C. C. Hegna, UW-CPTC-13, August,1997.

[3] W. Park et al., Phys. Rev. Lett.**75**, 507 (1995).

[4] F. L. Waelbroeck, Phys. Fluids B **1**, 2372 (1989).

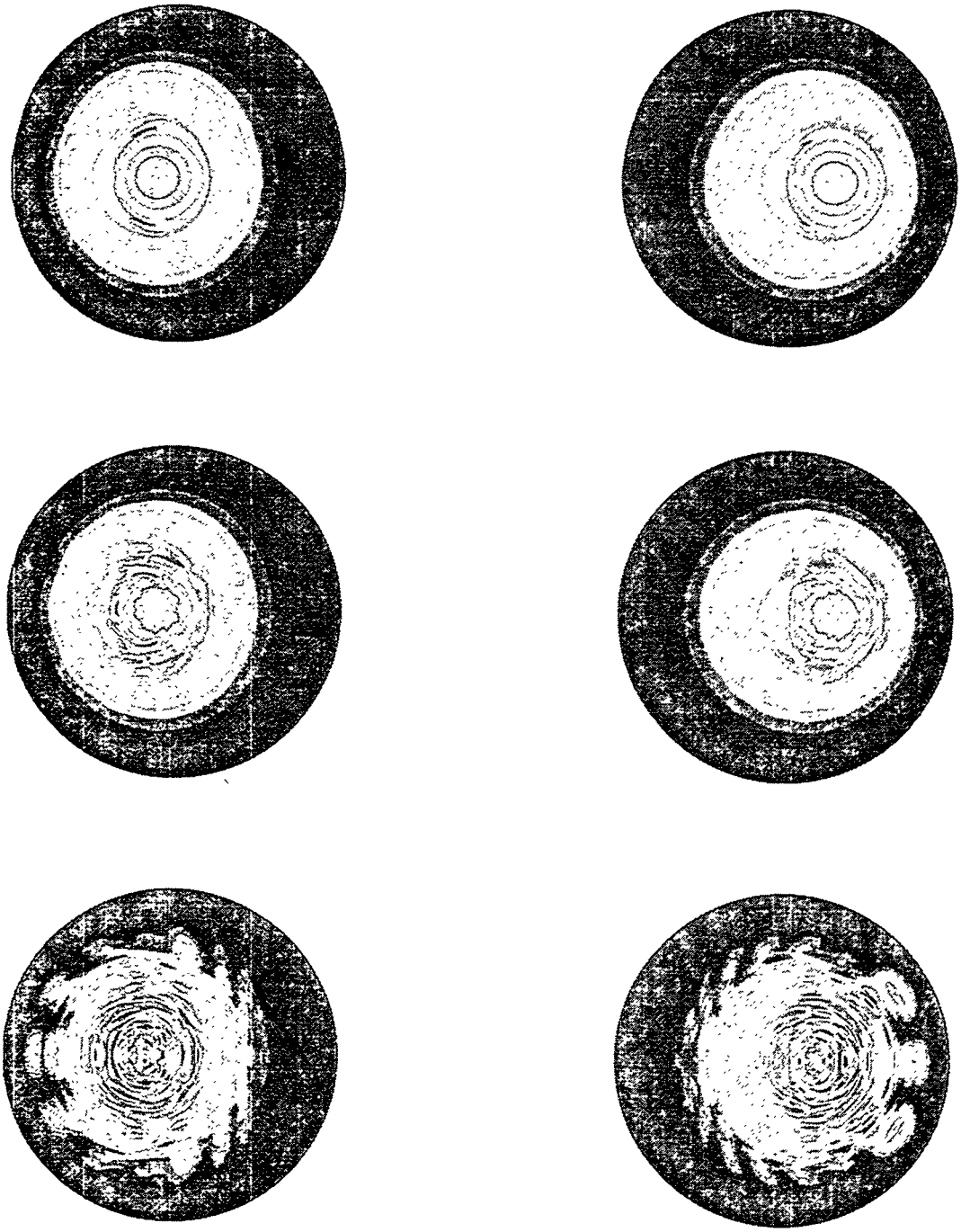

Figure 1: Pressure contours in the absence of finite parallel diffusion. At $t = 1400\tau_a$,$t = 1440\tau_a$, $t = 1480\tau_a$. To the left is at a toroidal angle $\zeta = \pi$. To the right is at $\zeta = 0$.

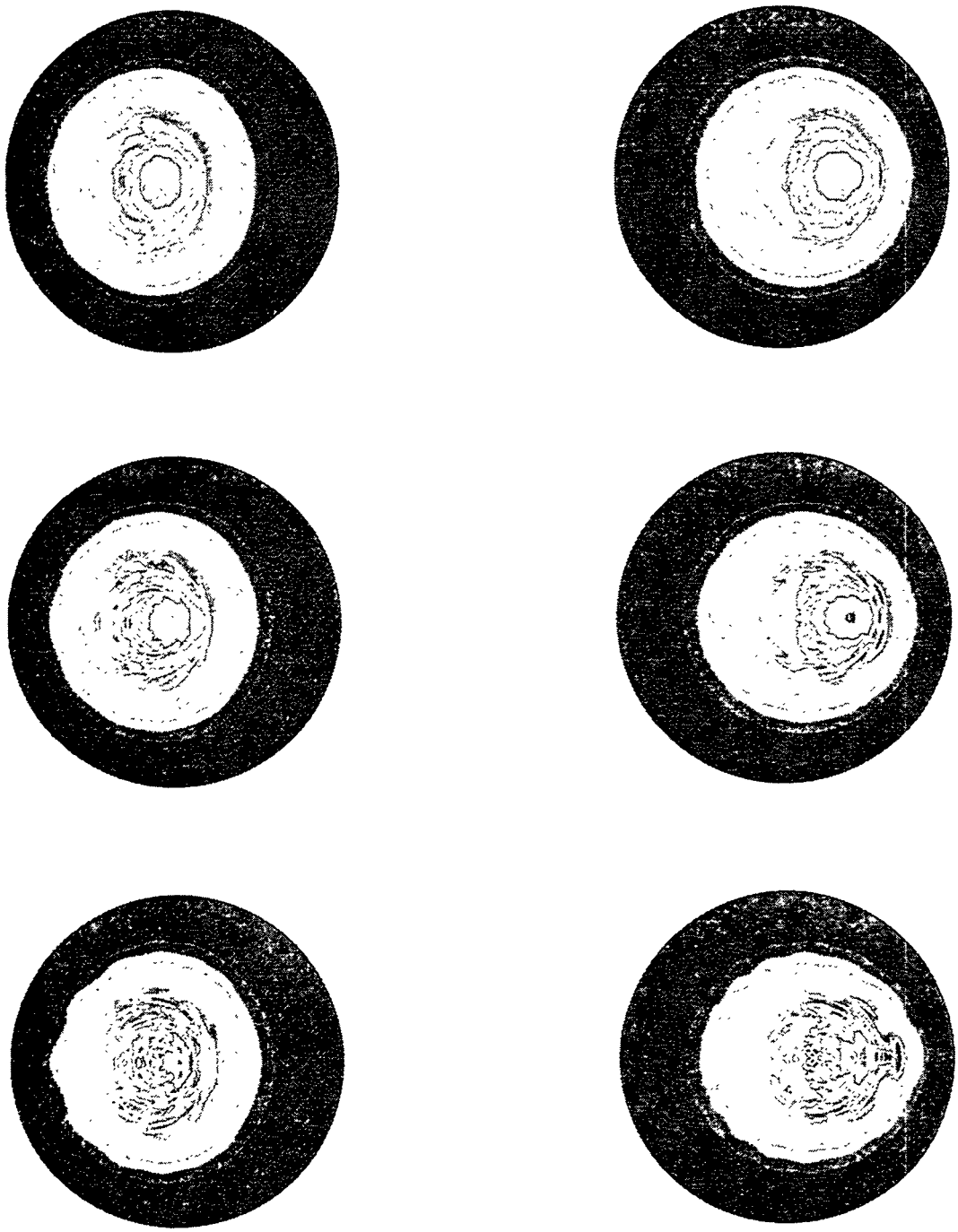

Figure 2: Pressure contours in the presence of finite parallel diffusion. At $t = 1445\tau_a$,$t = 1450\tau_a$, $t = 1455\tau_a$.

Hybrid Fluid/Kinetic Model For Parallel Heat Conduction

J.D. Callen, C.C. Hegna, and E.D. Held
University of Wisconsin, Madison, WI 53706-1687

Abstract

It is argued that in order to use fluid-like equations to model low frequency ($\omega < \nu$) phenomena such as neoclassical tearing modes in low collisionality ($\nu < \omega_b$) tokamak plasmas, a Chapman-Enskog-like approach is most appropriate for developing an equation for the kinetic distortion (F) of the distribution function whose velocity-space moments lead to the needed fluid moment closure relations. Further, parallel heat conduction in a long collision mean free path regime can be described through a combination of a reduced phase space Chapman-Enskog-like approach for the kinetics and a multiple-time-scale analysis for the fluid and kinetic equations.

The objective of hybrid fluid/kinetic descriptions of toroidal plasmas is to capture all of the essential physics for particular phenomena of interest within a fluid moment (MHD-like) model. To do so, one must determine and use appropriate closure moments in the fluid moment equations being considered. For example, an appropriate stress tensor Π is required to complete the specification of a momentum balance equation while both the stress tensor and the heat flux $\mathbf{q}$ are required to complete an energy balance equation. Once appropriate closures are employed, the full power of fluid moment computational models can be employed to describe the inherently three dimensional character of macroscopic, nonlinear phenomena in toroidal plasmas.

The needed closure moments are determined from particular velocity-space moments of the kinetic distribution function and represent the effects of higher order (than the fluid moments that are being kept) distortions F of the distribution function away from the lowest order distribution function which is typically taken to be Maxwellian. If the closure moments are exact, then the fluid moment description provides an exact description of the plasma dynamics. However, in practice approximations must be made to solve for the kinetic distortion F and these lead to only approximate closure moments — if the kinetic equation was exactly soluble one should just solve it rather than try to develop a hybrid fluid/kinetic model! Further, a hybrid computational model will be more efficient (faster) than a fully kinetic approach only if the appropriate kinetic distortion F and hence the needed closure moments can be adequately determined in a reduced phase space so that the computational effort required for determining F and the needed closure moments is significantly less than what would be required for a complete computational kinetic solution.

The most widely used closure relations are those derived by Braginskii [1], which are applicable to small gyroradius, collisional plasmas where the collision frequency is much less than the gyrofrequency ($\nu < \omega_c$), and the gradient scale lengths perpendicular and parallel to the magnetic field are long compared to the gyroradius ($\rho_i \nabla_\perp < 1$) and collision mean free path ($\lambda \nabla_\parallel < 1$), respectively. While a small gyroradius approximation is usually appropriate for the perpendicular processes, the collision mean free path in present tokamak and other toroidally confined "hot" plasmas is usually long compared to the parallel gradient scale length — usually by two or more orders of magnitude! Thus, an important challenge is to develop closure relations that take account of long collision mean free path ("collisionless") phenomena along magnetic field lines in toroidal plasmas.

Time scales are also important. In particular, in toroidal plasmas the phenomena of interest usually take place on time scales long compared to those associated with the plasma frequency

($1/\omega_{pe} \sim 10^{-12}$ s), ion gyrofrequency ($1/\omega_{ci} \sim 10^{-8}$ s), compressional-Alfvèn wave frequency ($1/k_\perp c_A \sim 10^{-7}$ s), and electron bounce motion ($1/\omega_{be} \sim 3 \times 10^{-7}$ s). Equilibrium on these various time scales implies that we can adopt the following respective approximations and descriptions: quasineutrality ($\nabla \cdot \mathbf{J} = 0$), drift-kinetics or gyrokinetics (if $k_\perp \rho_i \sim 1$), MHD force balance (Grad-Shafranov) equilibrium and reduced MHD descriptions [2], and distinguishing between trapped versus untrapped electrons in an electron kinetic distortion F that is constant along magnetic field lines to lowest order.

The frequencies of the phenomena that need to be included, say to describe the nonlinear evolution of neoclassical MHD tearing modes [3], are: shear-Alfvèn waves ($1/k_\parallel c_A \sim 10^{-6}$ s), electron collisions ($1/\nu_e \sim 10^{-5}$ s), diamagnetic flow frequency ($1/\omega_* \sim 3 \times 10^{-4}$ s), ion collisions ($1/\nu_i \sim 10^{-3}$ s), and finally tearing mode growth in the Rutherford [4] regime [$w/(\Delta' \eta/\mu_0) \sim 10^{-1}$ s]. The corresponding physical phenomena on these various time scales are, respectively: shear-Alfvèn waves and instabilities, a parallel Ohm's law that includes the parallel electron viscous force and hence the bootstrap current, drift waves, ion poloidal flow damping, and the nonlinear evolution of resistive and neoclassical MHD tearing-mode-induced magnetic islands (hopefully to a benign saturation). Note in particular that since in typical toroidal plasmas of interest the electron thermal speed significantly exceeds the Alfvèn speed ($v_{Te}/c_A = \sqrt{\beta_e m_i/m_e} > 1$), electrons travel faster than shear-Alfvèn waves along magnetic field lines. Thus, the (collisionless) free-streaming of untrapped electrons over the magnetic mirrors and wave-particle resonances (where $\omega \sim k_\parallel \langle v_\parallel \rangle$) along magnetic field lines should be taken into account in lowest order in the determination of the kinetic distortion F. The higher order determination of the kinetic distortion F for the electrons needs to simultaneously include the effects of shear-Alfvèn waves, collisions, wave-particle resonances, diamagnetic flow frequencies, and tearing mode evolution which all take place on longer time scales where the distinction between trapped and untrapped electrons has already been established. In particular, on the longer time scale, electron collisions act on the untrapped electrons to induce a parallel viscous force (and viscous heat force in the heat flux equation) that acts to damp poloidal electron flows (and heat fluxes) in the toroidal plasma and thereby leads to the bootstrap current and other effects.

Because one is typically interested in phenomena whose temporal variations are slow compared to the electron collision frequency ($1/\omega > 1/\nu_e \sim 10^{-5}$ s), the lowest order electron distribution function can be taken to be a "dynamic Maxwellian" — a Maxwellian whose parameters are the density $n(\mathbf{x}, t)$, temperature $T(\mathbf{x}, t)$, and flow velocity $\mathbf{V}(\mathbf{x}, t)$ in which the dependence on the time t explicitly allows these "parameters" to be determined by the fluid moment equations ($\partial n/\partial t = \cdots$, etc.). Using a dynamic Maxwellian (instead of the static Maxwellian on an equilibrium flux surface as is commonly used in drift-wave instability studies) as the Ansatz for the lowest order distribution function, one then uses a Chapman-Enskog-like approach [5,6] to develop an equation for the kinetic distortion F. This approach provides [6] a rigorous procedure for including wave-particle resonance (i.e., Landau damping [7]) processes, including nonlinear effects [8], within a fluid-like description. It also provides a procedure for deductively determining [9] the neoclassical parallel viscous force closure $\langle B \cdot \nabla \cdot \Pi \rangle$ [10], including the variation [11] of the parallel viscous force within a magnetic flux surface, $B \cdot \nabla \cdot \Pi$.

The neoclassical parallel viscous force closures currently used in neoclassical MHD [12] capture the poloidal flow damping and bootstrap current effects in "low collisionality" ($\nu < \omega_b$) plasmas. These effects are caused by the drag effect of collisions with trapped particles on the untrapped particles, which free-stream over the magnetic mirrors along field lines and carry the flow. However, a number of approximations are used in their derivation: the plasma is assumed to be quasistatic or evolving

slowly ($\omega < \nu$); flows within a flux surface are assumed to be much larger than those across flux surfaces ($V_\theta \gg V_r$); no potential variation is allowed for along magnetic field lines ($k_\| R_0 q \ll 1$); and finite banana width and gyroradius effects are neglected ($1 \gg k_\perp \Delta r_T > k_\perp \rho$). One would like to remove these limitations to provide a comprehensive description of low frequency processes. However, since further analytic progress seems difficult, a general Chapman-Enskog-like kinetic equation should be developed that incorporates all these effects (or most, like in [13]). A numerical procedure similar to that by Morris et al. [14] could then be used to solve the resultant kinetic equation.

A major problem that has emerged in the simulation [15] of neoclassical tearing modes is the incorporation of parallel electron heat conduction effects. This effect causes the electron temperature to be constant, at least to lowest order, along the magnetic field lines and in particular the helical magnetic flux surfaces within a slowly evolving nonlinear magnetic island. The main problem with a purely fluid description is that, because the parallel electron heat diffusivity is many orders of magnitude greater than the perpendicular heat diffusivity ($\chi_\|/\chi_\perp > 10^8$), it severely limits the maximum time step in the temperature (or pressure) evolution equation. Also, the nature of the equilibration along field lines in low collisionality plasmas where the Braginskii closures are no longer valid is not clear. In a kinetic description the problems are that the electron thermal speed is typically greater than the Alfvèn speed ($v_{Te} > c_A$) so the electron free-streaming along field lines becomes the shortest time scale process, and the irreversible collisional equilibration of the electron temperature along field lines requires following the electrons over many magnetic mirrors along field lines. In either description, the problem is that the time step is shortened considerably for neoclassical tearing modes compared to regular tearing modes and hence the simulation time becomes prohibitively long and/or numerical errors arise in the characterization of the magnetic island structure [15].

What is needed to make comprehensive neoclassical tearing mode (and other low collisionality magnetized plasma) simulations practicable is to develop a new, temporally efficient procedure for incorporating electron parallel free-streaming and heat conduction in the simulations. We suggest that to develop an efficient approach one needs to make simultaneous and similar orderings in the fluid moment and kinetic (for F) equations. For the problematic electron free-streaming and heat conduction effects, this would imply that for equilibrium on the electron bounce time scale ($\sim 1/\omega_{be} \sim 3 \times 10^{-7}$ s) in the fluid description the electron temperature is taken to be constant along magnetic field lines (including those within a magnetic island), and in the kinetic description the lowest order electron distribution function is taken to be constant along field lines. Further, on this time scale the difference between untrapped and trapped particles becomes evident, and the first-order electron distribution using a Chapman-Enskog-like approach exhibits the free-streaming of electrons over the poloidal magnetic mirrors — $F = (v_\| B - \langle v_\| B \rangle / f_c)\ (U_\theta + (2q_\theta/5p) L_1^{(3/2)})\ (m/T) f_M + h$ in which U_θ and q_θ are the poloidal flow and heat fluxes, and h is the non-free-streaming and hence nonadiabatic kinetic distortion. Then, in next order one would solve (probably numerically) the residual bounce-averaged kinetic equation which would include collisional pitch-angle scattering, wave-particle resonance, etc. effects. The parallel viscous force and heat stress would then be obtained from the stress velocity-space moments of h. The parallel heat flux would thus be determined on the first order (collisional) time scale. Further, on this same time scale the slight departures of the electron temperature from constancy on magnetic field lines would be determined. Then, these results would be incorporated into the numerical solutions of the reduced MHD equations [2] whose time advance is effectively on the same time scale. Thus, the procedure suggested would attempt to analytically incorporate the rapid electron free-streaming and constancy

of temperature along magnetic field lines in the lowest order description. and then only need to advance the kinetic and fluid moment equations on the slower time scales that correspond to the electron collisional, shear-Alfvèn, and wave-particle resonance time scales.

In summary, we suggest that the most natural procedure for developing a hybrid fluid/kinetic model for describing "slow" ($\omega < \nu$) processes in low collisionality ($\nu \ll \omega_b$, banana-regime) toroidal plasmas is via a Chapman-Enskog-like approach that provides a rigorous procedure for determining the kinetic distortion F and corresponding closure moments that are consistent with the (nonlinear) fluid moment equations. Because for toroidal, magnetized plasmas of interest $v_{Te} > c_A$, the parallel electron streaming over the magnetic mirrors along field lines needs to be accurately described before proceeding to the shear-Alfvèn time scale that underlies numerical solutions of the reduced MHD equations [2]. We suggest that to develop an appropriate computational algorithm we will need to simultaneously order and solve both the fluid moment and kinetic equations — first make the electron temperature constant along magnetic field lines and bounce-average the kinetic equation, then advance the resultant fluid moment and kinetic equations on the shear-Alfvèn and collisional time scales.

ACKNOWLEDGEMENT. The authors gratefully acknowledge useful discussions with D.C. Barnes, T.A. Gianakon and M.C. Zarnstorff. This research was supported by DoE grant DE-FG02-86ER53218.

References

[1] S.I. Braginskii, in **Reviews of Plasma Physics** (Consultants Bureau, NY, 1965), Vol. I, p. 205.
[2] H.R. Strauss, Phys. Fluids **19**, 134 (1976); **20**, 1354 (1979); B.V. Waddell et al., Phys. Fluids **22**, 896 (1979); S.E. Kruger, C.C. Hegna, J.D. Callen, "Generalized Reduced MHD Equations," UW-CPTC 98-8, July 1998 (to be published in Phys. Plasmas).
[3] Z. Chang, J.D. Callen, E.D. Fredrickson, R.V. Budny, C.C. Hegna, K.M. McGuire, M.C. Zarnstorff and TFTR Group, Phys. Rev. Lett. **74**, 4663 (1995). See also references cited therein and [12], [13], and [15].
[4] P.H. Rutherford, Phys. Fluids **16**, 1903 (1973).
[5] J.P. Wang and J.D. Callen, Phys. Fluids B **5**, 1139 (1992).
[6] Z. Chang and J.D. Callen, Phys. Fluids B **5**, 1167 (1992); 1182 (1992).
[7] G.W. Hammett and F.W. Perkins, Phys. Rev. Lett. **64**, 3019 (1990).
[8] N. Mattor and S.E. Parker, Phys. Rev. Lett. **79**, 3419 (1997); N.Mattor, Phys. Plasmas **5**, 1822 (1998)
[9] J.D. Callen, Z. Chang and J.P. Wang, "Direct derivation of Neoclassical Viscosity Coefficients in Tokamaks," Paper at EPS Meeting, Amsterdam, 25-29 June 1990.
[10] S.P. Hirshman and D.J. Sigmar, Nuclear Fusion **21**, 1079 (1981).
[11] J.P. Wang and J.D. Callen, Phys. Fluids B **5**, 3207 (1993).
[12] J.D. Callen et al., "Neoclassical MHD Equations, Instabilities and Transport in Tokamaks," in **Plasma Physics and Controlled Nuclear Fusion Research 1986** (IAEA, Vienna, 1987), Vol. II, p. 157.
[13] H. Wilson, J.W. Connor, R.J. Hastie, and C.C. Hegna, Phys. Plasmas **3**, 248 (1996).
[14] R.C. Morris, M.G. Haines, and R.J. Hastie, Phys. Plasmas **3**, 4513 (1996).
[15] T.A. Gianakon, C.C. Hegna, J.D. Callen, Phys. Plasmas **3**, 4637 (1996).

Poloidal and Toroidal Rotation in Tokamak Plasmas

L. Sugiyama (MIT)

See

"The M3D Prodect Simulation Studies"
Wonchull Park, E.V. Belova, G.Y. Fu, H.R. Strauss, and L.E. Sugiyama

3D HYBRID SIMULATIONS WITH GYROKINETIC PARTICLE IONS AND FLUID ELECTRONS

E. V. Belova. W. Park, G. Y. Fu (PPPL)
H. R. Strauss (NYU) and L. E. Sugiyama (MIT)

Introduction

The previous hybrid MHD/particle model (*MH3D-K* code) represented energetic ions as gyrokinetic (or drift-kinetic) particles coupled to MHD equations using the pressure or current coupling scheme [1-3]. A small energetic to bulk ion density ratio was assumed, $n_h/n_b \ll 1$, allowing the neglect of the energetic ion perpendicular inertia in the momentum equation and the use of MHD Ohm's law $\mathbf{E} = -\mathbf{v}_b \times \mathbf{B}$. A generalization of this model in which all ions are treated as gyrokinetic/drift-kinetic particles and fluid description is used for the electron dynamics is considered in this paper.

The standard approach in gyrokinetic particle simulations is to solve the gyrokinetic Poisson equation, including the polarization term [4] (for the electrostatic case), and the parallel Ampere law (when low β electromagnetic perturbations are considered [5]). In a more general case of fully electromagnetic perturbations the gyrokinetic Poisson equation should be modified to include contributions from both $A_{\|}$ and $A_{\perp}$ and the perpendicular Ampere law has to be added to complete the system of equations. The alternative approach is to use Ohm's law (electron momentum equation) to find the electric field. In this method, which is typical for hybrid simulation with fully kinetic particle ions and fluid electrons, a calculation of the ion perpendicular velocity will be needed. Unlike the previous hybrid model [1-3], where the bulk plasma provides most of the inertia and the gyrokinetic ions contribute only to the plasma beta, it is important to include ion perpendicular inertia (polarization current) when all ions are gyrokinetic particles.

In the pressure coupling scheme, discussed here, the ion perpendicular inertia is retained by calculating the ion fluid velocity from momentum equation, in which the ion pressure tensor is calculated using particle simulations. The nonlinear δf method [2] is employed to reduce the numerical noise level. The model is applied to the study of the effect of thermal particle ions on the stability of internal kink mode, and the simulation results are compared

with 1-fluid and 2-fluid MHD simulations.

Gyrokinetic/2-fluid hybrid scheme

In the pressure coupling scheme the ion fluid velocity is calculated by solving momentum equation, and the calculated ion fluid velocity is used in the Ohm's law, which includes the Hall term and the electron pressure gradient; quasineutrality is assumed:

$$\frac{\partial(\rho_i \mathbf{V}_i)}{\partial t} = -\nabla p_e - \nabla \cdot \mathbf{P}_i^{CGL} - \nabla \cdot \mathbf{\Pi}_{gi} + \mathbf{J} \times \mathbf{B}$$

$$\partial \mathbf{B}/\partial t = -\nabla \times \mathbf{E}, \quad \mathbf{E} = -\mathbf{V}_e \times \mathbf{B} - \frac{1}{en_e}\nabla p_e, \quad n_i = n_e$$

Here the ion pressure is taken to be in CGL form and the gyroviscous part of the stress tensor is calculated in order to take into account the diamagnetic effects. The ion pressure is calculated from gyrokinetic particles, whereas the gyroviscous tensor, $\mathbf{\Pi}_g$, can be calculated from particles or taken into account in a fluid way [6,7].

The ions are pushed using the guiding center equations of motion:

$$\dot{\mathbf{X}} = \frac{1}{B}\left[\mathbf{B}^* U + \hat{\mathbf{b}} \times (\mu \nabla B - \mathbf{E})\right],$$

$$\dot{U} = -\frac{1}{B}\mathbf{B}^* \cdot (\mu \nabla B - \mathbf{E}), \quad \dot{\mu} = 0,$$

where $(\mathbf{X}, U, \mu, \theta)$ - gyro-center coordinates, and $\mathbf{B}^* = \mathbf{B} + U\hat{\mathbf{b}} \times (\hat{\mathbf{b}} \cdot \nabla \hat{\mathbf{b}})$.

The equilibrium distribution function, $F_0 = F_0(p_\phi, \mu, \epsilon)$ is a function of the integrals of motion: $p_\phi = R\hat{\phi} \cdot \mathbf{A}^* = \psi + URb_\phi$ (toroidal angular momentum) and $\epsilon = \mu B + m_i U^2/2$. For the thermal ions: $F_0 = exp(-p_\phi/\psi_0 - \epsilon/T)$ chosen.

Calculation of gyroviscous force

The gyroviscous terms appear naturally in the gyrokinetic description, when the transformation from the gyro-center to particle coordinates is made in the pressure integral; however, this approach requires the ion Larmor radius to be resolved in the simulations. In order to include the diamagnetic effects in the drift-kinetic formulation, the small ion Larmor radius expansion can be made in the pressure tensor integral, which gives the expression for the gyroviscous stress tensor in terms of the gyrofluid moments

$$\mathbf{P}_i^{CGL} = \|U^2\|\hat{\mathbf{b}}\hat{\mathbf{b}} + \|\mu B\|(\mathbf{I} - \hat{\mathbf{b}}\hat{\mathbf{b}})$$

$$\begin{aligned}\nabla\cdot\mathbf{\Pi}_{gi} &= \hat{\mathbf{b}}\times\nabla\left(\nabla_{\|}\|\mu U\|\right)\\ &+ \nabla_{\perp}\left(\nabla_{\perp}^{2}\|\mu^{2}\|/4-3\chi_{\perp}/2+n\mathbf{V}_{*i}\cdot\mathbf{V}_{E}\right)\\ &+ \nabla_{\|}\left(\nabla_{\perp}^{2}\|U^{2}\mu\|/2B-\chi_{\|}-\chi_{\perp}\right),\end{aligned}$$

where

$$\chi_{\perp(\|)}=-\frac{p_{\perp(\|)}}{B}\hat{\mathbf{b}}\cdot\nabla\times\mathbf{V}_{E},\quad \|*\|=\int(*)F_{i}\,d^{3}\mathrm{v},\quad F_{i}=F(\mathbf{X},U,\mu,t),\quad \hat{\mathbf{b}}=\mathbf{B}/B.$$

The above expressions were obtained by performing the transformation from particle variables to guiding-center coordinates in the stress tensor integral, and then expressing the guiding-center distribution function in terms of the gyro-center distribution function F. After the gyroaverages were calculated, the small $(k_{\perp}\rho)$ expansion was made, using ordering:

$$\frac{\rho_{i}}{L}\sim\frac{\omega}{\omega_{ci}}\sim\frac{k_{\|}}{k_{\perp}}\sim\varepsilon,\quad \varepsilon\leq(k_{\perp}\rho)^{2}<1$$

Here $\mathbf{P}^{CGL}$ is zero order (in ε) part of the ion stress tensor $\mathbf{P}$, and gyroviscous tensor $\mathbf{\Pi}_{g}$ is defined to include FLR corrections to $\mathbf{P}$ (up to $O(k_{\perp}^{2}\rho^{2})$) plus inertial term: $\mathbf{\Pi}_{g}\equiv\mathbf{P}-\mathbf{P}^{CGL}$. The diagonal corrections, which represent the difference between the gyrofluid moments (calculated in the code) and the particle-fluid moments are also taken into account in $\mathbf{\Pi}_{g}$. The gyroviscous part of the stress tensor was derived assuming electrostatic perturbation and uniform background magnetic field.

Comparison with fluid calculations

The FLR corrections to ion pressure tensor and, especially, the off-diagonal terms are important for correct drift Alfven wave dispersion, the diamagnetic stabilization of resistive 1/1 mode, and the problem of plasma rotation in a tokamak. It is well known that the inclusion of the gyroviscous force $\nabla\cdot\mathbf{\Pi}_{g}$ leads to the gyroviscous cancellations and corrections in the momentum equation. In order to show that our results agree with the previous fluid calculations [6,7], we find the relation between $\mathbf{\Pi}_{g}$ and the conventional definition of gyroviscous stress tensor $\boldsymbol{\pi}_{g}=\mathbf{P}-\mathbf{p}^{CGL}-\rho\mathbf{VV}$:

$$\begin{aligned}\mathbf{\Pi}_{g}=\boldsymbol{\pi}_{g}+\rho\mathbf{VV} &+ \left(p_{\perp}-\|\,\mu B\,\|-\rho V_{\perp}^{2}/2\right)(\mathbf{I}-\hat{\mathbf{b}}\hat{\mathbf{b}})\\ &+ \left(p_{\|}-\|\,U^{2}\,\|-\rho V_{\|}^{2}\right)\hat{\mathbf{b}}\hat{\mathbf{b}}\end{aligned}$$

Then calculating the difference between gyrofluid and particle-fluid moments, and truncating higher order moments as follows: $\| \mu U \| \approx p_\perp V_\| / B$ and $\|\mu^2\| \approx 2p_\perp^2 / nB^2$, we obtain

$$\nabla \cdot \boldsymbol{\pi}_g = -\left(n\mathbf{V}_* \cdot \nabla\right)\mathbf{V} + \nabla_\perp \tilde{\chi}/2 + p_\perp \hat{\mathbf{b}} \times \nabla \left(\nabla_\| V_\|\right)$$

where $\tilde{\chi} = -p\hat{\mathbf{b}} \cdot \nabla \times \mathbf{V}/B$. This result agrees with calculations of gyroviscous force in [6,8].

Simulation of internal kink mode

The above gyrokinetic/2-fluid hybrid scheme has been applied to the study of an ideal internal m=1/n=1 kink mode in toroidal geometry, assuming zero electron pressure, for the following set of parameters: the aspect ratio $R/a = 3.0$, $q(0) = 0.6$, $q(a) = 2.3$, and the ion beta $\beta = 0.06 - 0.1$. The linear growth rates and mode structure obtained in the particle simulations were compared with the results of 1-fluid MHD and 2-fluid (including gyroviscous force) MHD simulations with same equilibrium density and pressure profiles. The ideal MHD growth rate for this beta range was: $\gamma\left(\tau_A^{-1}\right)$ =0.035 - 0.053, whereas the growth rate, calculated in the particle simulations, was γ =0.017 - 0.042. Thus, in agreement with analytical estimates, the effect of particle ions on internal kink mode is stabilizing. The obtained linear growth rate was approximately the same, when the gyroviscous effects were also included, probably, because the diamagnetic frequency was small compared to γ. However, there was much better agreement in terms of the mode structure between particle simulations and 2-fluid MHD simulations with the gyroviscous force included. The particle simulations with smaller growth rates proved to be much more expensive, because better resolution in particle poloidal grid, and therefore, larger number of particles and smaller time steps were needed to resolve the mode structure.

References

1. W. Park et al., Phys. Fluids B **4**, 2033 (1992).
2. G.Y. Fu and W. Park, Phys. Rev. Lett. **74**, 1594 (1995).
3. E.V. Belova et al., J. Comput. Phys., 136, 324 (1997).
4. W.W. Lee, Phys. Fluids, **26**, 556 (1983).
5. T.S. Hahm, W.W. Lee and A. Brizard, Phys. Fluids, **31**, 1940 (1988).
6. Z. Chang and J. D. Callen, Phys. Fluids B4, 1766, (1992)
7. R. D. Hazeltine and J.D. Meiss, Phys. Rep. **121**, 1 (1985).
8. A. Brizard, Phys. Fluids B **4**, 1213 (1992).

Workshop on Nonlinear MHD and Extended MHD

Kinetic and Fluid Models of Drift Wave Turbulence

F. Jenko and B. Scott

Max-Planck-Institut für Plasmaphysik
EURATOM Assoziation, D-85748 Garching

Comprehensive models for tokamak edge turbulence require at least two essential ingredients, namely electron drift waves and toroidal ITG modes. Beyond that one might need to include additional modes. The current work focuses on kinetic drift wave turbulence, leaving the simultaneous kinetic treatment of electron and warm ion dynamics to future work.

Tokamak H-mode edge turbulence can be characterized by two very important properties. First, the electrons are only weakly collisional, i.e. the electron thermal transit frequency $\nu_t = v_{te}/qR$ exceeds the electron collision frequency ν_e,

$$\nu_t > \nu_e,$$

such that Landau damping effects in the parallel electron dynamics need to be retained. Second, the turbulent fluctuations are electromagnetic, i.e. the plasma beta $\beta_e = 4\pi p_e/B^2$ is greater than the electron to ion mass ratio $\mu_e = m_e/M_i$,

$$\beta_e > \mu_e.$$

Therefore the parallel component $A_\parallel$ of the vector potential has to be kept along with the scalar potential ϕ, and the drift waves become drift Alfvén waves.

We have carried out numerical simulations of drift wave turbulence in this weakly collisional, electromagnetic regime using drift-kinetic electrons and cold ions in three-dimensional sheared slab geometry. The model equations are

$$\frac{df_e}{dt} + v_\parallel \nabla_\parallel f_e - \frac{eE_\parallel}{m_e}\frac{\partial f_e}{\partial v_\parallel} = \frac{\nu_e}{(v/v_{te})^3}\frac{\partial}{\partial \zeta}(1-\zeta^2)\frac{\partial f_e}{\partial \zeta} \equiv C[f_e] \qquad (1)$$

for the electrons where $C[f_e]$ is a Lorentz collision operator and $\zeta = v_\parallel/v$,

$$nM_i\frac{du_\parallel}{dt} = neE_\parallel + nM_i\mu_\parallel\nabla_\parallel^2 u_\parallel - \int m_e v_\parallel C[f_e]\, d^3v \qquad (2)$$

for momentum-conserving parallel ion dynamics, and

$$en\rho_s^2\frac{d}{dt}\nabla_\perp^2\left(\frac{e\phi}{T_{e0}}\right) = \nabla_\parallel\left(enu_\parallel - \int ev_\parallel f_e\, d^3v\right) \qquad (3)$$

describing quasineutrality which is maintained by the ion polarization current, so that $\nabla \cdot \mathbf{J} = 0$ for the total current. This condition determines the time

dependence of ϕ and hence the $\mathbf{E}\times\mathbf{B}$ drift velocity $\mathbf{v}_E$. The advective derivative is given by

$$\frac{d}{dt} = \frac{\partial}{\partial t} + \mathbf{v}_E \cdot \nabla_\perp ,$$

and magnetic shear modifies the equations through the perpendicular Laplacian

$$\nabla_\perp^2 = \left(\frac{\partial}{\partial x} + \hat{s} z \frac{\partial}{\partial y}\right)^2 + \left(\frac{\partial}{\partial y}\right)^2$$

and the parallel boundary condition

$$S(x, y, z + 2\pi) = S(x, y - xz\hat{s}, z)$$

for any scalar quantity S where we have normalized the parallel coordinate z to qR. The perpendicular boundary conditions are taken to be periodic.

Under drift ordering, we split the distribution function f_e into a background Maxwellian and a fluctuating part,

$$f_e(x, y, z; \zeta, v; t) = f_m(x; v) + \tilde{f}(x, y, z; \zeta, v; t).$$

For $\beta \ll 1$, the electromagnetic field fluctuations are given by

$$\tilde{\mathbf{B}}_\perp = \nabla \tilde{A}_\parallel \times \mathbf{b}_0 , \quad \tilde{B}_\parallel = 0$$

where $\mathbf{b}_0$ is the unit vector in the direction of the unperturbed magnetic field, and

$$\tilde{\mathbf{E}}_\perp = -\nabla_\perp \tilde{\phi}, \quad \tilde{E}_\parallel = -\nabla_\parallel \tilde{\phi} - \frac{1}{c}\frac{\partial \tilde{A}_\parallel}{\partial t},$$

supplemented by the parallel component of Ampère's law,

$$\tilde{J}_\parallel = -\frac{c}{4\pi} \nabla_\perp^2 \tilde{A}_\parallel .$$

The parallel derivatives are taken along the perturbed field lines,

$$\nabla_\parallel = \frac{\partial}{\partial z} + \frac{\tilde{\mathbf{B}}_\perp}{B_0} \cdot \nabla_\perp ,$$

retaining the effects of magnetic flutter.

The most important dimensionless parameters controlling the kinetic Alfvén wave speeds are

$$\hat{\beta} = \beta_e \left(\frac{qR}{L_\perp}\right)^2 = \left(\frac{c_s/L_\perp}{v_A/qR}\right)^2 \qquad \text{and} \qquad \hat{\mu} = \mu_e \left(\frac{qR}{L_\perp}\right)^2 = \left(\frac{c_s/L_\perp}{v_{te}/qR}\right)^2 .$$

Other parameters are

$$\nu = \frac{\nu_e}{c_s/L_\perp}, \quad \eta_e = \frac{L_n}{L_{T_e}}, \quad \hat{s} = \frac{r}{q}\frac{\partial q}{\partial r}.$$

The gyro-Bohm normalized transport coefficients D and χ are functions of these dimensionless parameters, e.g. $D = D(\hat{\beta}, \hat{\mu}, \nu, \eta_e, \hat{s})$.

The equations (1-3) are solved numerically using a Vlasov method, i.e. representing all dynamic variables by their values on a grid in (phase) space and replacing the differential operators by finite-difference approximations. Due to the five-dimensional distribution function the code needs much memory and CPU time. Therefore it has been parallelized and runs on a massively parallel distributed memory machine, a Cray T3E.

The resulting turbulence is driven by a collisionless version of the well-known resistive nonlinear instability [1, 2] with $\mathbf{E}\times\mathbf{B}$ drift induced energy transfer in $k_\parallel$ space. Whereas linear electron Landau damping provides a free-energy sink for the turbulent system (playing the same role as collisionality in resistive drift wave models), nonlinear electron Landau damping - associated with parallel acceleration through the velocity space nonlinearity $\tilde{E}_\parallel \partial_{v_\parallel} \tilde{f}$ - leads to parallel trapping of electrons in wells of the electrostatic potential. Simulation results in the electrostatic limit ($\hat{\beta} \to 0$) indicate that the transport level is reduced significantly for low shear ($\hat{s} < 1$), but for moderate or high shear ($\hat{s} > 1$) the suppression is only about 10% or less, i.e. of the order of the statistical uncertainties observed in the simulations [3]. Thus in a tokamak edge ($r/a > 0.8$), where generally $\hat{s} > 1$, nonlinear electron Landau damping does not seriously affect collisionless drift wave turbulence.

In the electromagnetic regime, one of the most interesting questions is the scaling of particle and heat transport with $\hat{\beta}$. If one chooses $\hat{\mu} = 10$ (which is a typical tokamak edge value) and holds it fixed, one sees a decrease in transport with rising $\hat{\beta}$ in the collisionless regime but the opposite trend in the collisional regime. The latter finding is in agreement with results from an electromagnetic Landau-fluid model [4]. As long as the magnetic flutter terms in the parallel derivatives are switched off, both models yield a rise in transport with $\hat{\beta}$ in all collisionality regimes. In this case, the magnetic induction term in $\tilde{E}_\parallel$ is the only electromagnetic effect present. Thus the magnetic flutter terms in the parallel derivatives are crucial for computations of drift Alfvén turbulence, as they stabilize the system and reduce the turbulent transport. In the collisionless limit they can even override the destabilizing power of the magnetic induction. Whereas magnetic flutter doesn't contribute much to the cross-field transport directly, it can still change the dynamic equilibrium of the turbulence and thus have an impact on the observed ExB transport level. The fluid model has shown that in the collisional regime the strong β dependence of the drift Alfvén turbulence carries over to a system with warm ions and thus ITG modes [5]. Classical ITG modes alone have only a relatively weak β dependence through the magnetic equilibrium configuration. If the same is true in the weakly collisional case, there might be a possible connection between the β scaling of drift Alfvén turbulence and the L-H transition which is surprisingly well described by the relation $\beta = \mu_e$ in several machines [6].

As mentioned earlier, the tokamak H-mode edge is weakly collisional so that Landau damping effects need to be retained. Besides the kinetic approach outlined in this paper, one can also try to construct Landau fluid models which extend the usual fluid models into the collisionless regime and allow for a description of the plasma which is much less costly both analytically and numerically. Whereas there has been some success in recent years concerning electrostatic systems, the construction of electromagnetic Landau fluid models for tokamak edge turbulence is a more difficult task. Unfortunately, magnetic flutter is in the way of dealing with $k_{||}$ dependent dissipative terms like in the approaches of Hammett and Perkins [7] or Chang and Callen [8]. Before making a Fourier transform to $k_{||}$ space one would have to follow all quantities along the perturbed field lines from one end of the flux tube to the other. As this process seems very hard to implement, alternative types of Landau fluid models are called for which circumvent this problem. They are a necessary step on the way towards more comprehensive tokamak edge transport models.

*

References

[1] B. D. Scott, Phys. Rev. Lett. **65**, 3289 (1990).

[2] D. Biskamp and A. Zeiler, Phys. Rev. Lett. **74**, 706 (1995).

[3] F. Jenko and B. D. Scott, submitted to Phys. Rev. Lett.

[4] B. D. Scott, Plasma Phys. Contr. Fusion **39**, 1635 (1997).

[5] B. D. Scott, Contrib. Plasma Phys. **38**, 171 (1998).

[6] Yu. Igitkhanov *et al.*, *IAEA Technical Committee Meeting on H-Mode Physics*, Kloster Seeon, Germany, 1997

[7] G. W. Hammett and F. W. Perkins, Phys. Rev. Lett. **64**, 3019 (1990).

[8] Z. Chang and J. D. Callen, Phys. Fluids B **4**, 1167 (1992).

MHD STABILITY OF THE MHH2 STELLARATOR

P.R. Garabedian
New York University, Courant Institute of Mathematical Sciences
New York, New York 10012

The NSTAB code provides a computer implementation of the variational principle of magnetohydrodynamics. Excellent resolution is obtained by combining a spectral representation in the toroidal and poloidal angles with a low order, but exceptionally accurate, finite difference scheme in the radial direction. Conservation form of the magnetostatics equations is used to capture islands and current sheets effectively on crude grids. This method enables one to discuss global stability by analyzing bifurcated solutions of the equilibrium problem. We apply it to investigate the physics of the MHH2 stellarator, whose magnetic structure has a remarkable property of quasi-axial symmetry.

In our formulation of the problem the toroidal equilibria calculated by the variational principle lend themselves in a natural way to the representation

$$\mathbf{B} \;=\; \nabla s \times \nabla\theta \;=\; \nabla\phi + \zeta\nabla s$$

of the magnetic field in terms of Clebsch potentials. It is convenient to choose the toroidal flux s as a radial coordinate and to renormalize θ and ϕ so they become poloidal and toroidal angles on each flux surface s =const. In this invariant coordinate system we can expand the magnetic field strength in a Fourier series

$$\frac{1}{B^2} = \sum B_{mn}\cos(m\theta - [n - \iota m]\phi) \;,$$

where ι is the rotational transform. The coefficients B_{mn}, which are functions of s alone, comprise the magnetic spectrum of the equilibrium [ ]. The axial symmetry property of the MHH2 stellarator simply states that the terms with $n \neq 0$ are relatively small. More specifically, in practical cases they contribute little more than 1% to the total field strength, which suffices to guarantee confinement times comparable to those in standard tokamaks.

Formal integration yields the Fourier expansion

$$\lambda = \frac{\mathbf{J}\cdot\mathbf{B}}{B^2} = p'\sum \frac{mB_{mn}}{n - \iota m}\cos(m\theta - [n - \iota m]\phi) \;,$$

provided that the relevant differentiations can be performed. The small denominators that appear on the right exhibit dramatically the resonances that occur at rational surfaces where $\iota = n/m$. The resulting failure of convergence of the series is important

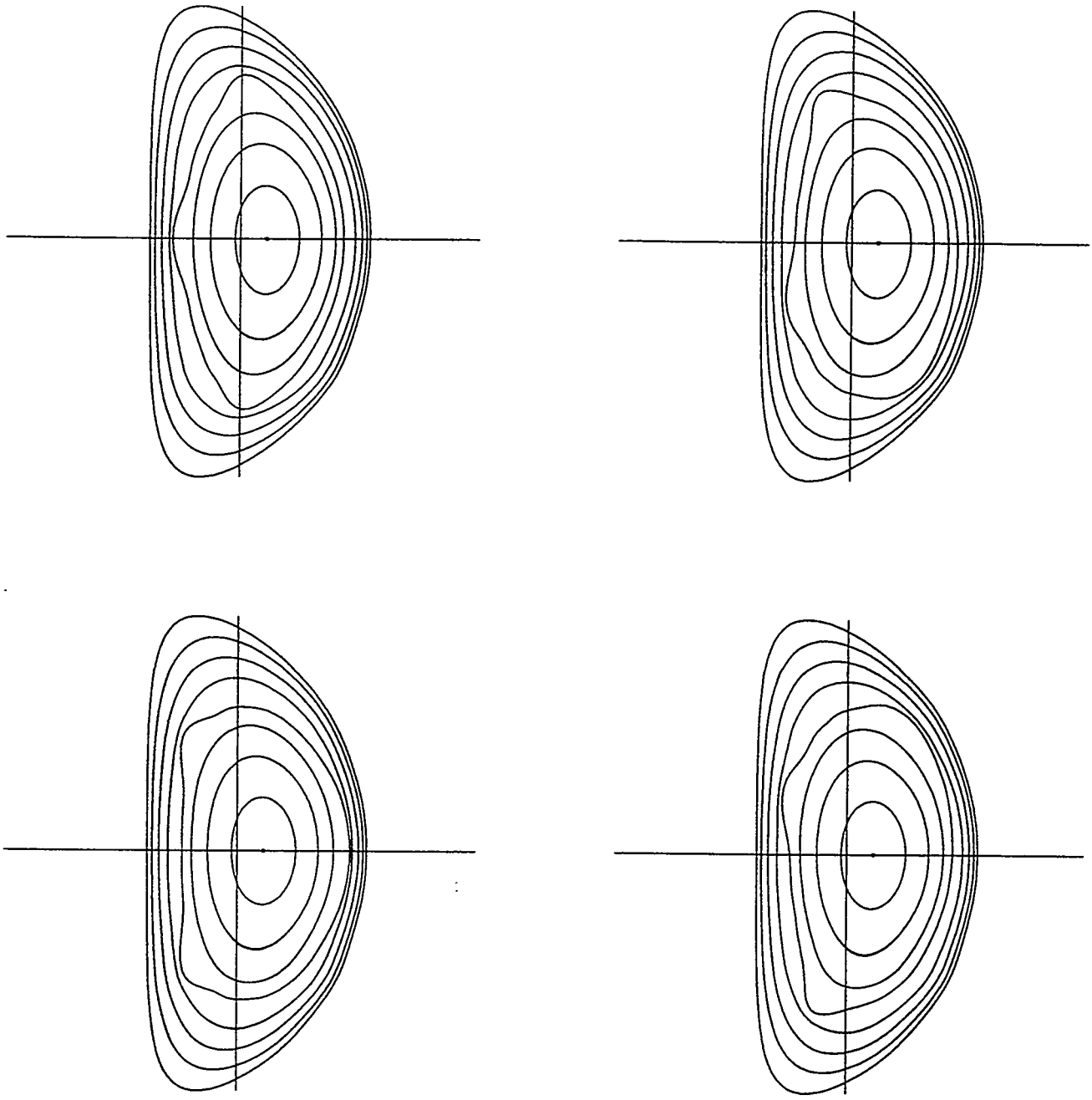

NSTAB calculation of four Poincaré sections of the flux surfaces of a spherical tokamak showing how the code captures small islands at the resonance $\iota = 2/3$ in a bifurcated equilibrium without two-dimensional symmetry.

in the KAM theory, which shows that smooth solutions of the equilibrium problem cannot exist in three dimensions because the coefficients B_{mn} do not in general vanish.

The success of stellarator experiments makes it imperative to to find a formulation of the toroidal equilibrium problem in three dimensions that overcomes the difficulty about nonexistence of continuously differentiable solutions. The answer furnished by the NSTAB code is to calculate weak solutions determined by equations in a conservation form that is associated with the variational principle of magnetohydrodynamics and requires less differentiation. Because the dependence of the magnetic field on the poloidal and toroidal angles is relatively smooth, good resolution in those variables can be obtained by the spectral method. However, in the radial coordinate s we use a special finite difference scheme that captures islands accurately on grids with a mesh size comparable to the island width. Detailed calculations have demonstrated that this mathematical model simulates the physics of the plasma remarkably well.

Even for tokamaks with two-dimensional solutions we have been able to find a variety of bifurcated equilibria that have islands breaking the axial symmetry. An example is displayed in Fig. 1 for a spherical tokamak of aspect ratio $A = 1.8$ with rotational transform in the interval $1.1 \geq \iota \geq 0.2$. To draw correct physical conclusions it is necessary to allow for this kind of complication in the structure of the magnetic surfaces.

The NSTAB code solves the magnetostatic equations numerically by means of an accelerated method of steepest descent. In significantly unstable cases the potential energy has access to a lower level and a second bifurcated solution can be constructed. Calculation of the bifurcated equilibrium is facilitated by introducing a perturbation in the equations that is associated with some mode deemed to be dangerous. A valid measure of instability is convergence to a bifurcated solution different from the original equilibrium after the perturbation has been removed. That is a criterion relatively free of details about the specific formulation of the variational principle that is used.

Our most successful analysis of stability for the MHH2 configuration has resulted from performing perturbations that break the stellarator symmetry of the equilibrium over a single period characterized by the appearance of exclusively cosine terms in the Fourier series for $1/B^2$. A bifurcated solution found this way is displayed in Fig. 2 for a mode triggered by trigonometric functions with $m = 6$, $n = 2$. The instability has been induced by adding bootstrap current so that the rotational transform ι over one field period falls from 0.32 at the magnetic axis down to 0.26 at the edge of the plasma. Observe that the asymmetric ripple of the bifurcated flux surfaces is concentrated in a region of bad curvature and has a ballooning structure that follows the magnetic lines.

Since the variational principle of magnetohydrodynamics furnishes an accepted mathematical model of stability in plasma physics, the key issue in our approach becomes the numerical accuracy of the NSTAB code. Extensive comparisons with two-dimensional theory and with laboratory measurements indicate that NSTAB computations of the kind we have described do have the necessary resolution, and the results seem to provide a realistic simulation of the most essential phenomena. More specif-

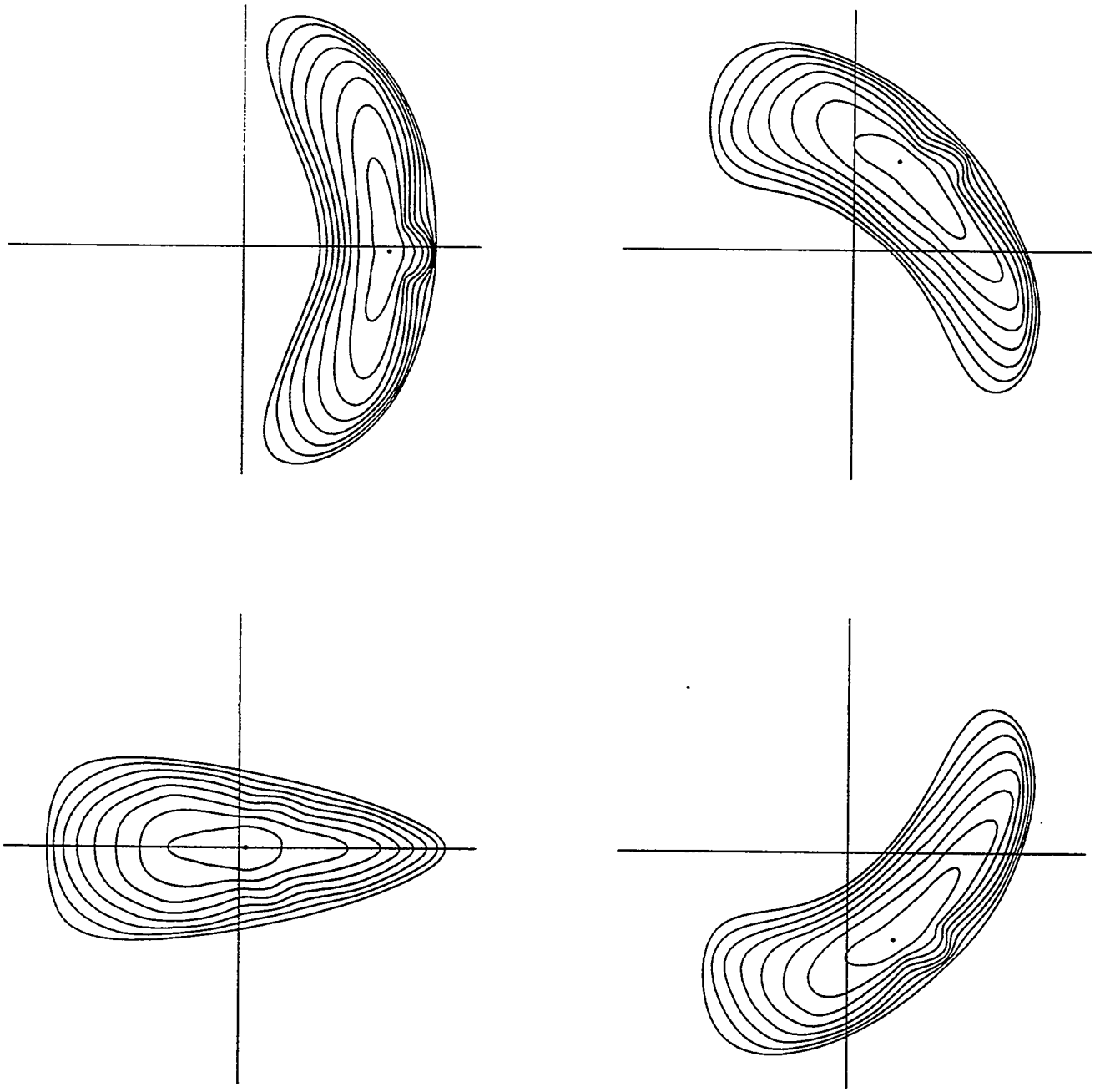

Poincaré sections of the magnetic surfaces over one field period of a bifurcated MHH2 equilibrium with bootstrap current at an average β of 5.5 percent. The solution exhibits ripple without the stellarator symmetry of the plasma boundary. This establishes instability of a ballooning mode localized in the region of bad curvature, but extending globally along the radius.

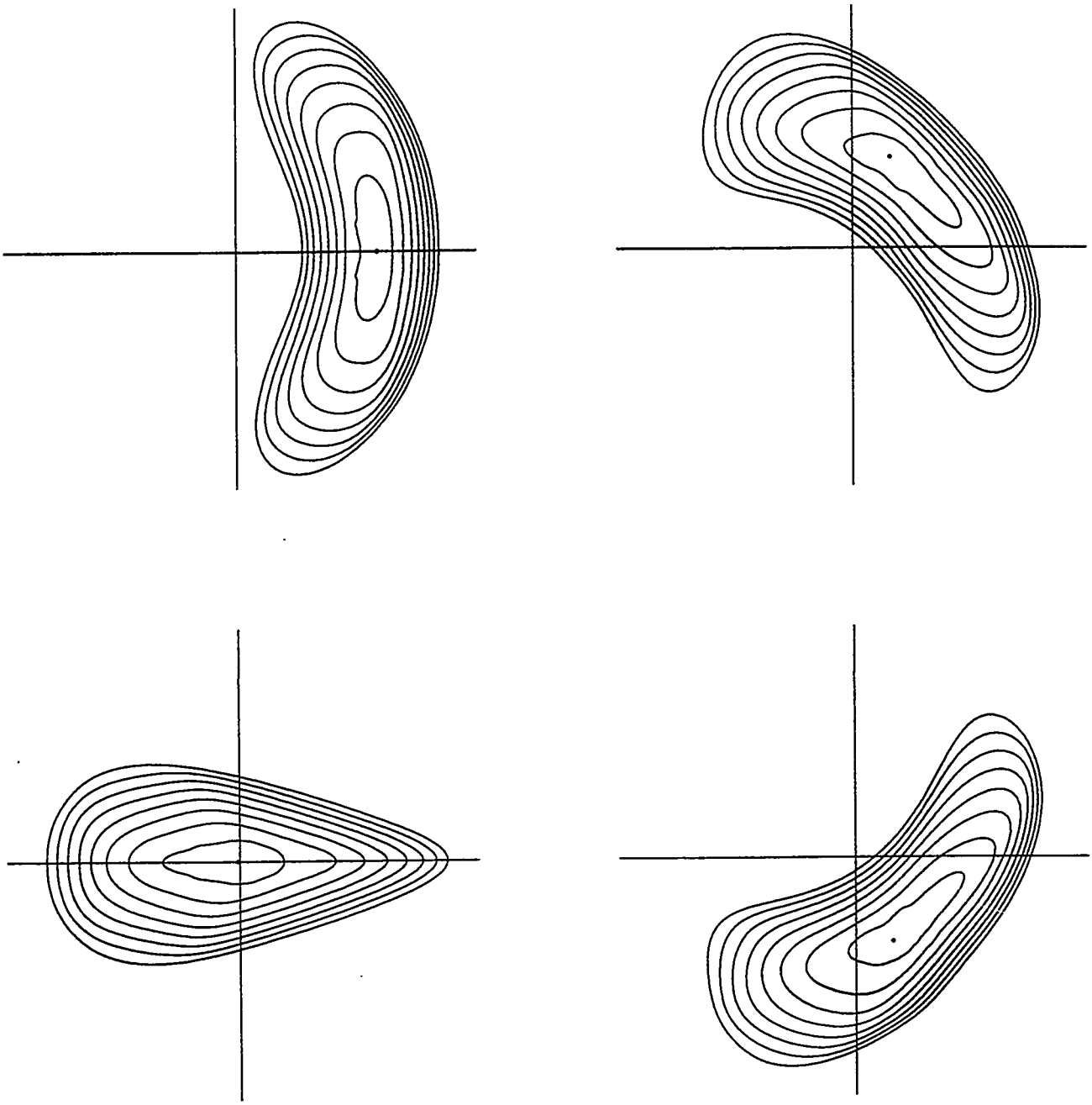

Poincaré sections over one field period of an optimized MHH2 equilibrium at an average β of 2.0 percent. The magnetic surfaces of the solution have no ripple after perturbations have decayed, which establishes nonlinear stability in this case.

ically, it has been found that recent estimates of β limits for the Compact Helical System (CHS) experiment in Japan agree quite well with our prediction of nonlinear stability for modes of moderately high order.

Not all of the methods that have been proposed to solve the three-dimensional equilibrium problem are equally successful. In the PIES code the interface between a region of nested surfaces and an island region of constant pressure ought to be a flux surface, but the surface current there due to discontinuity of the magnetic field at any sharp boundary is neglected. Many of the linearized stability calculations build on runs of the VMEC code that are not fully converged. The VMEC method is closely related to ours, but a compatibility condition associated with nonuniqueness of the Clebsch representations of $\mathbf{B}$ is treated in a more complicated fashion that makes it unclear whether the discrete system of equations in the code actually has an exact solution. Also, a question of reliability arises about the evaluation of derivatives occurring in the linearized problem whose existence is placed in doubt by the KAM theorem.

The Mercier local stabiity criterion can be written in the form

$$\Omega = C_1 \iota'^2 + C_2 p' V'' + C_3 p'^2 + C_4 p'^2 \Big[\Big(\int \lambda dF \Big)^2 - \int dF \int \lambda^2 dF \Big] \; > \; 0 \; ,$$

where the coefficients C_k and the measure dF have been defined elsewhere, and $-V''$ is the magnetic well. Because of Schwarz's inequality the contribution in square brackets is always negative. The divergence of the Fourier series for the parallel current λ in fully three-dimensional equilibria therefore signifies that the criterion will predict instability if too many terms are included in the calculation. However, the series has been truncated in the NSTAB code to arrive at a more practical version that turns out to be well correlated for stellarators with our nonlinear analysis. In this context a physically more realistic criterion for stability seems to be $\Omega > -.01$.

The ballooning mode algorithms that have been presented in the literature involve a system of ordinary differential equations obtained from an asymptotic expansion of perturbations in the neighborhood of some magnetic line. The Mercier criterion emerges as a limiting case of the ballooning theory, so the latter may also predict erroneous instability for stellarators if it is carried to an extreme. Of more concern, however, are computations restricted to a shorter arc of the magnetic line. The answer depends on the length of the arc, so results can become biased to reach a preconceived conclusion. Moreover, the ordinary differential equations for ballooning modes have features in common with linearized stability theory, which means that derivatives have to be computed that may not exist. In our work we bypass these difficulties by appealing in the last analysis to the nonlinear stability test based on an NSTAB computation of bifurcated solutions, and we only rely on our truncated version of the Mercier criterion for quick parameter searches. On the whole the Mercier results seem to fit stellarator data well, while the ballooning theory is preferred for tokamaks.

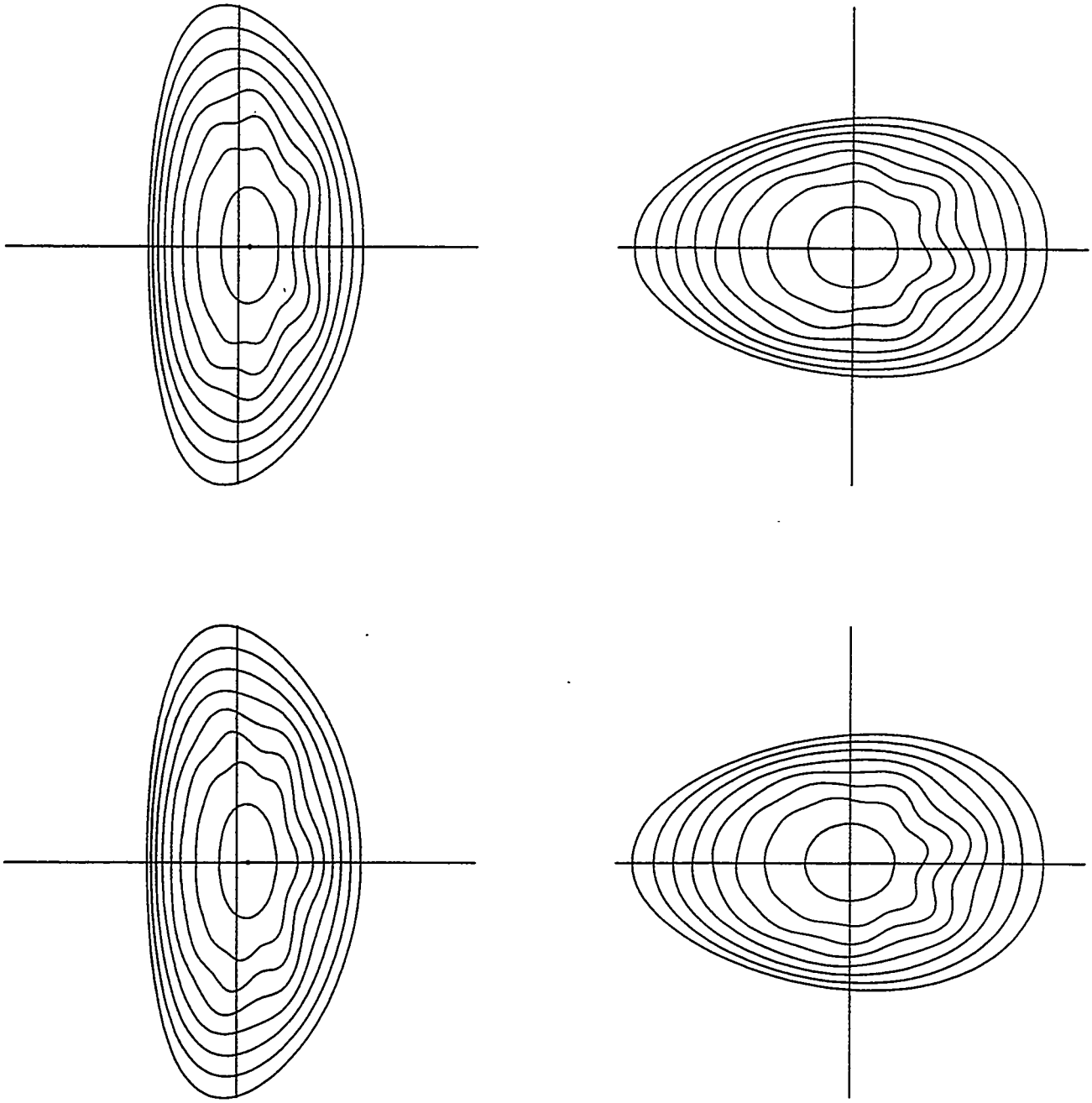

Poincaré map of the flux surfaces over two field periods of a bifurcated CHS equilibrium at a β of 1.0 percent. The solution has ripple without the symmetry of the plasma boundary, showing instability. The result agrees with experimental estimates of the β limit when the axis is shifted inward, and it serves to validate the nonlinear theory.

Acknowledgments

This work has been supported by the United States Department of Energy under Grant DE-FG02-86ER53223 and by the National Science Foundation under Grant DMS-9420499. We wish to express our appreciation for helpful discussions with Frances Bauer.

References

1. D. Anderson and P. Garabedian, A stellarator configuration for reactor studies, Nucl. Fusion **34** (1994) 881–885.

2. F. Bauer, O. Betancourt and P. Garabedian, *Magnetohydrodynamic Equilibrium and Stability of Stellarators*, Springer-Verlag, New York, 1984.

3. P. Garabedian, Stellarators with the magnetic symmetry of a tokamak, Phys. Plasmas **3** (1996) 2483–2485.

4. P. Garabedian, Three-dimensional tokamak equilibria and stellarators with two-dimensional magnetic symmetry, Plasma Phys. Control. Fusion **39** (1997) B129–B134.

5. S. Hirshman and O. Betancourt, Preconditioned descent algorithm for rapid calculations of magnetohydrodynamic equilibria, J. Comp. Phys. **96** (1991) 99–109.

6. S. Okamura *et al.*, Compatibility of drift orbit optimization with MHD stability in CHS, to be published.

7. A. Reiman and H. Greenside, Computation of zero β three-dimensional equilibria with magnetic islands, J. Comp. Phys. **87** (1990) 349–365.

8. M. Taylor, A high performance spectral code for nonlinear MHD stability, J. Comp. Phys. **110** (1994) 407–418.

Nonlinear tearing mode study using the "almost ideal magnetohydrodynamics (MHD)" constraint

C. Ren,[1] T. H. Jensen,[2] and J. D. Callen[1]

[1] *University of Wisconsin-Madison, Madison, WI 53706-1687*

[2] *General Atomics, P.O. Box 85608, San Diego, CA 92186-9784*

The tearing mode [1] is an important resistive magnetohydrodynamics (MHD) mode. It perturbs the initial equilibrium magnetic flux surfaces through magnetic field line reconnection to form new flux surfaces with magnetic islands. In the study of the tearing mode, usually the initial equilibria are one dimensional with two ignorable coordinates and the perturbed equilibria are two dimensional with one ignorable coordinate. Therefore, magnetic flux surfaces exist for both the initial and the perturbed equilibria. The tearing mode can be linearly unstable and its growth saturates at a finite amplitude [2]. The neoclassical tearing mode theory [3] shows that the mode can be nonlinearly driven by the bootstrap current even when it is linearly stable to the classical tearing mode. It is important to study the nonlinear behavior of the tearing mode.

As an intrinsically nonlinear approach, the use of the "almost ideal MHD" constraint [4] is suited to study the nonlinear properties of the tearing mode. In this paper, as a validation of the method, we study two characteristics of the tearing mode using the "almost ideal MHD" constraint: 1) the linear stability condition for the initial one dimensional equilibrium; and 2) the final saturation level for the unstable case. In this work, we only consider the simplest case where no gradient of pressure or current density exists at the mode resonant surface.

The tearing mode cannot exist under the ideal MHD constraint, which does not permit changes in flux surface topology. On the other hand, it is well known that the ideal MHD constraint is violated only in a narrow region near the mode resonant surface, where the magnetic field is perpendicular to the wave vector of the mode. The "almost ideal MHD" constraint is a relaxation of the ideal MHD constraint to allow such local changes of the flux surface topology [4].

In principle one can find many equilibria with islands which are associated with the initial one dimensional equilibrium through the "almost ideal MHD" constraint. In general these island equilibria have a singular current at the X-point of the islands. Depending on the sign of this singular current, the equilibrium evolves, on the tearing mode time scale, in the direction of either increasing or decreasing the island width. We are interested in an equilibrium where the singular current is zero and therefore is a final stationary state. If such a final equilibrium is found to include an island, then the initial equilibrium is presumed to be tearing-mode unstable and the island width of the final state is the saturation width. If no possible final state with an island is found, then the initial equilibrium is tearing-mode stable. Because we do not use any small amplitude expansion, this approach is intrinsically nonlinear.

We now use an example to illustrate the application of the "almost ideal MHD" constraint to the problem of tearing mode stability and saturation. We consider a simple case where there is no pressure gradient, $\nabla p = 0$. Then, the force-balance equation for the equilibrium is just $\mathbf{J} \times \mathbf{B} = 0$. We use Cartesian coordinates where $\hat{\mathbf{z}}$ is an ignorable coordinate ($\partial/\partial z = 0$) for both the initial and final equilibrium. The initial equilibrium is also independent of y. The magnetic field $\mathbf{B}$ is expressed through functions $B_z(x, y)$ and $\psi(x, y)$ as

$$\mathbf{B} = B_z \hat{\mathbf{z}} + \nabla\psi \times \hat{\mathbf{z}}.$$

Then, the force-balance equation becomes

$$\nabla^2\psi + B_z \frac{dB_z}{d\psi} = 0 \tag{1}$$

with $B_z = B_z(\psi)$. Equation (1) determines both the initial and final equilibrium, once $B_z(\psi)$ and the boundary conditions are given.

The ideal MHD constraint for this $\nabla p = 0$ case can be represented by requiring that the B_z flux enclosed by a flux surface $\psi = \psi_1$,

$$\phi(\psi_1) = \int B_z S[\psi(x, y) - \psi_1] dx dy,$$

$$S[u] = \begin{cases} 1 & u > 0 \\ 0 & u < 0, \end{cases}$$

be a conserved function. For simplicity, we consider the limit where $B_z \to \infty$, $B_z' \to 0$ and $B_z B_z'$ remains finite. Then, the conservation of $\phi(\psi)$ is equivalent to the incompressibility of the plasma. That is, the area enclosed by a flux surface remains constant; i.e.,

$$A(\psi_1) = \int S[\psi(x,y) - \psi_1] dx dy$$

is a conserved function.

To relax this constraint to the "almost ideal MHD" constraint, we only require a finite number of "moments" of $A(\psi)$ to be conserved. That is, the set of integrals,

$$g_n = \int G_n(\psi) dA, \quad n = 1, 2, \ldots, N,$$

where G_n is a set of base functions, are conserved. The base functions G_n should be sufficiently diverse in ψ-space. The number of base functions is finite to allow magnetic field line reconnection. When the number of base functions approaches infinity, the "almost ideal MHD" constraint approaches the ideal MHD constraint. So, formally, the "almost ideal MHD" constraint can be written as

$$g_{nf} = g_{ni}, \quad n = 1, 2, \ldots, N \tag{2}$$

where g_{nf} and g_{ni} are the integrals of the nth base function over the final and initial state, respectively. The set g_{ni} can be calculated from the given initial equilibrium and is the only information needed from it. Our goal is to find a final state $\psi(x,y)$ that satisfies both (1) and (2), by choosing the right form of $B_z B_z'$.

Finding the exact solution of Eqs. (1) and (2) is difficult. Therefore, a numerical algorithm is used to find an approximate solution. The function $B_z B_z'$ is parameterized by a set of parameters p_m, $m = 1, 2, \ldots, M$. The aim is to adjust p_m's to minimize the quantity $Q = \sum_{n=1}^{N} (g_{nf} - g_{ni})^2$.

Obviously, the initial island-free equilibrium itself is always a possible final state. A successful algorithm must find a final state other than the initial one if the initial equilibrium is unstable to the tearing mode. It can be proved that the Jacobi algorithm used to solve Eq. (1) converges to the initial state only if the Δ', the tearing mode stability parameter [1], of the initial state is negative. So if the initial equilibrium is tearing-mode unstable ($\Delta' > 0$), the algorithm moves the solution away from it towards a different equilibrium.

We will show that the stability criterion is the same as the linear "Δ' theory" [1] and give the saturation width for an unstable initial equilibrium. The saturation level is found to be smaller than that estimated from $\Delta'(W_{sat}) = 0$ [2].

One of the authors (CR) is grateful for the hospitality and help he has received at General Atomics. This work is supported by US DoE grant no. DE-FG02-92ER54139.

---

[1] H. P. Furth, J. Killeen, and M. N. Rosenbluth, Phys. Fluids **6**, 459 (1963).

[2] B. Carerras, B. V. Waddell and H. R. Hicks, Nucl. Fusion **19**, 1423 (1979).

[3] W. X. Qu and J. D. Callen, University of Wisconsin Report No. UWPR-85-5, 1985 (unpublished). Copies may be ordered from the National Technical Information Service, Virginia 22161 (NTIS Document No. DE86008946). The price is $12.50 plus a $3.00 handling fee. All orders must be prepaid.; R. Carrera, R. D. Hazeltine and M. Kotschenreuther, Phys. Fluids **29**, 899 (1986); J. D. Callen, W. X. Qu, K. D. Siebert, B. A. Carreras, K. C. Shaing and D. A. Spong, in *Plasma Physics and Controlled Nuclear Fusion Research* Kyoto, 1986 (IAEA, Vienna, 1987), Vol. 2 p.157.

[4] T. H. Jensen, A. W. Leonard, R. J. La Haye and M. S. Chu, Phys. Fluids B **3**, 1650 (1991); T. H. Jensen and K. H. Finken, Bull. American Physical Society **41**, 3098 (1996).

[5] T. H. Jensen and W. B. Thomson, Phys. Fluids **30**, 3052 (1987).

Chuang Ren

General Atomics

MS 13-321

PO Box 85608

San Diego, CA 92186-9784

Phone: 619-455-4023; Fax: 619-455-3586

E-mail: ren@cptc.wisc.edu

LINEAR AND NONLINEAR ASPECTS OF MHD USING A TWO-FLUID, GLOBAL ELECTROMAGNETIC CODE- CUTIE

A. Thyagaraja
UKAEA, Fusion, Culham Science Centre, Abingdon, OX14 3DB, UK.
(UKAEA/Euratom Fusion Association)

1. INTRODUCTION AND SUMMARY

The CUTIE turbulence simulation code developed at Culham is a global code based on an electromagnetic two-fluid plasma model. It has been used to study nonlinear saturation of fast-particle driven Alfvén eigenmodes by the mode coupling mechanism and shows that typical saturation amplitudes due to 'nonlinear radiation damping' are comparable with those due to well-known velocity-space mechanisms. Other studies involving global (ie low m, n tearing or ballooning type) modes show that large-scale coherent modes can exist in a saturated state. Although developed primarily to study turbulent transport processes on a 'mesoscale', the code offers interesting numerical insights into the nature of saturation mechanisms. Recent linear and nonlinear analytic studies which may throw some light on nonlinear saturation and global mode structure will also be briefly described. Critical issues arising in global computational studies for the 'arithmetical tokamak physicist' will be discussed with relevant examples.

2. THEORETICAL MODEL

The linear and nonlinear theory of TAE modes [1, 2, 3] has been studied extensively in the literature using the ideal MHD model for the evolution of the electromagnetic potentials as well as kinetic formulations (eg. the drift or gyrokinetic equation) to obtain the alpha particle kinetic reponse. An electromagnetic turbulence code which was previously developed at Culham[4], has been adapted to study the problem of the nonlinear evolution of TAE's. In this paper, results of this work are briefly summarized. The two-fluid model is used with a kinetic linear response for the alphas but including both linear and nonlinear background plasma effects. This is similar in spirit to the work of Vlad *et al*[7] in that we explore the consequences of the nonlinear mode coupling as a possible saturation mechanism. In a recent analytical study based on a compressible model, we showed[8] that, in principle, nonlinear coupling can be effective in damping TAE modes if the amplitude of the drive is large enough, and can be as significant as velocity-space effects previously discussed in the literature[9]. Here we show the effect of damped shear Alfvén waves coupled nonlinearly to the TAE in an *incompressible* model. For definiteness, the alpha-drive is kept fixed to distinguish the present mechanism from the usual one where the mode growth leads to alpha re-distribution resulting in saturation[1, 9].

Although the CUTIE code solves the reduced two-fluid system[4, 5], in the present work TAE's are described in the MHD framework[6]. The diamagnetic terms of the alphas and the curvature terms are of course retained, as are the kink and line-bending terms of reduced MHD. The resulting equations are considerably simpler, although still strongly nonlinear and involve both dissipation and toroidal coupling. Even with these simplifications, the model contains visco-resistive tearing and ballooning modes and possesses, in suitable limits, all the generic properties of shear Alfvén waves in a

tokamak.

The typical forms of the vorticity and Ohm's law equations are:

$$\frac{\partial \Theta^*_{m,n}}{\partial t} + ik_\parallel V_A \nabla^2_\perp \psi_{m,n} = \frac{iV_A\psi_{m,n}}{r}\frac{d}{dr}\left(\frac{1}{r}\frac{d(r^2k_\parallel)}{dr}\right) + \Gamma_{\alpha m}\nabla^2_\perp \phi^*_{m,n} + \kappa_{m,n} \quad (1)$$

$$\frac{\partial \psi_{m,n}}{\partial t} + ik_\parallel V_A \phi^*_{m,n} = \frac{c^2\eta}{4\pi}\nabla^2_\perp \psi_{m,n} + \lambda_{m,n} \quad (2)$$

In the above equations we use the usual definitions of vorticity etc; appropriate non-dimensionalization is implied. We represent the drive due to alpha particles by a term on the RHS of the vorticity equation of the form[10] $\Gamma_{\alpha m}\nabla^2_\perp \phi^*_{m,n}$, where, $\Gamma_{\alpha m} = \frac{\beta_\alpha}{2R^2}\frac{V_A^2}{\omega_0}(\frac{\omega_{*\alpha m}}{\omega_0}-1)(R_{m+1}+R_{m-1}), \zeta_{m\pm1} = \omega/V_\alpha \mid k_{\parallel m\pm1} \mid, R_{m\pm1} = \pi^{1/2}\exp(-\zeta^2_{m\pm1})\zeta_{m\pm1}(\zeta^4_{m\pm1}+\zeta^2_{m\pm1}+1/2), V^2_\alpha = 2T_\alpha/m_\alpha$. The nonlinear, curvature and dissipation terms are in the $\kappa_{m,n}, \lambda_{m,n}$. A simple local dispersion relation gives the growth rate[1, 10], $\frac{\gamma}{\omega_0} = -(\beta_\alpha/4k^2_\parallel R^2)(1-\frac{\omega_{*\alpha}}{\omega_0})(R_{m+1}+R_{m-1})$ Since the R's are positive, instability occurs for $\omega_{*\alpha} > \omega_0$.

A novel solution scheme has been developed wherein the equations are split into mean(ie. flux-surface averaged) and fluctuating components interacting nonlinearly with each other. The linear terms describing shear Alfvén waves, tearing and ballooning modes are written in a 3×3 matrix form for each m, n Fourier component of $\delta\phi, \delta\psi, \Theta$. Nonlinear sources involving Jacobeans are finite-differenced using a conservative Arakawa scheme and evaluated in position-space and then transformed into Fourier space. The resulting implicit, unconditionally stable, matrix tridiagonal system is inverted by a Gaussian direct solver with provision for iterative improvement at a time-step. Curvature and toroidal effects are included in the fluctuation dynamics. A typical radial mesh size is $\Delta r \simeq a/200$ (ie. $0.5\rho_i$); up to 16 poloidal and 4 toroidal modes are employed. Time-steps resolve shear Alfvén frequencies ($\Delta t \simeq 1.25\times10^{-2}\mu$s).

3. TAE NONLINEAR SATURATION RESULTS

Linear code results support the simple analytic theory and also lead to quantitative estimates for the growth rate and linear eigenfunctions in agreement with the literature[1]. Typically, for $T_i \simeq 10$keV, $V_A \simeq 3000$km/s, $R = 3$m, $B \simeq 2$T, $T_\alpha \simeq 1$MeV, and alpha density scale-length, $L_{n\alpha} \simeq a/2$, the instability condition is readily satisfied. For experimental $\beta_\alpha \simeq 0.1\%$ we expect $\gamma/\omega_0 \simeq 10^{-3}$; in actual fact, we obtain a value around 3.5×10^{-2} for the $n = 1, m = -1, -2$ mode, corresponding to an e-folding time of about 100μs. It is interesting to note that in the strongest drive region there is evidence for highly oscillatory radial modes associated with vanishing parallel wave number. These appear to be closely related to those studied by Tsai and Chen[2]. We have continued the linear solution with the full nonlinear code using $-8 \le m \le 8, -2 \le n \le 2$, $\Delta t = 12.5$ nanosecs and $\Delta r = a/200$. As in the linear case, $\beta_\alpha = 0.003$. The nonlinear terms do not affect the solution until $\delta B/B \simeq 7.5\times10^{-6}$ at around 2.5 ms. The mode appears saturated at 3 ms with an amplitude level similar to observations in TFTR[3]. Figures 1,2 show the nonlinear evolution of the RMS vorticity and current density in the final stages of the run. The electrostatic potential, $e\phi/T \simeq 10^{-3}$ at this time. The calculation uses a 'sub-grid diffusivity' dependent on the calculated turbulence level[4]. This is about 1.4% of Bohm diffusivity, showing that saturation is due to nonlinear

mode coupling of the driven modes with the stable ones in the system.

4. DISCUSSION AND CONCLUSIONS

We have presented results on the nonlinear saturation of driven TAE modes via the mode coupling mechanism, keeping the linear alpha drive simple and fixed. The CUTIE code simulations agree with linear theory at low amplitude and with the results of Vlad *et al*[7] in the nonlinear phase, suggesting that this mechanism for mode saturation via position-space nonlinear mode coupling to stable branches (essentially a form of nonlinear radiation damping) is viable in existing devices such as JET. Saturation amplitudes are in the same range as those observed under similar experimental conditions [3]. It should therefore be considered in addition to the usual quasi-linear and velocity-space saturation mechanisms.

Recently[11] we have found that the continuous spectrum of ideal MHD must include the 'magnetosonic' branches which are stable but could profoundly modify both two-fluid nonlinear behaviour due to two close sound resonances and a fast branch which can have a global eigenfunction even in a cylinder. If a very small dissipation or electron inertia is present, it can be shown by elementary considerations of hyperbolic (ie advective systems with real characteristics) systems that the nonlinear excitation of continua implies a rapid 'cascade' to high k and consequent effective damping at a rate, $\tau_c^{-1} \propto (\nu)^{1/3}(\omega_A')^{2/3}$, where $\omega_A \simeq V_{\text{Alfven}}/a$ and ν is the (small) 'background' diffusivity. This damping rate is of course, far higher than that usually implied by the small diffusivity, and could play a vital role in saturating plasma turbulence. CUTIE has been used as a turbulent transport code and shows that finite β effects can be both stabilizing (via electromagnetic processes such as the aforementioned continua) and destabilizing (through the usual curvature/ballooning 'drive').

Some of the main problems facing the 'arithmetical tokamak physicist' in developing and using models such as CUTIE are listed: 1. Resolution of scales somewhat smaller than $c/\omega_{pe}, \rho_i$ at reasonable computing cost. 2. Time-resolution: $V_{\text{Alfven}}\Delta t \simeq \Delta r$. 3. 'Knudsen' corrections or correct 'gyrofluid' terms with *practical forms*. 4. Simultaneous, global equilibrium evolution and determination of 'quasi-linear' saturation 5. Physically motivated 'sub-grid turbulence' model, or equivalently, a summability method for the calculated Fourier series to avoid spurious Gibbs phenomena. 6. Need calculations valid on macroscopic time-scales (ie how is the 'chaos' to be averaged?). 7. Are the **mesoscale coherent structures** seen in the simulations 'real' or artefacts?

Results obtained thus far are encouraging, but many more careful studies and benchmarking in the fully global, nonlinear, EMHD regime between codes and comparisons of simulations with precision experiments are the way to further progress.

Acknowledgements: This work was funded jointly by the UK Dept. of Trade and Industry and Euratom.

References

[1] G.Y. Fu and J.W. Van Dam, Phys. Fluids B **1**, 1949 (1989).

[2] S-T. Tsai and L. Chen, Phys. Plasmas B **5**, 3284 (1993).

[3] R. Nazikian *et al*, Phys. Rev. Letters **78**, 2976 (1997).

[4] A. Thyagaraja, Proceedings of the International School of Plasma Physics, Piero Caldirola, Theory of Fusion Plasmas, Villa Monastero, Varenna, 155 (1996).

[5] A. Thyagaraja, C.N. Lashmore-Davies, W. Han and W-H. Yang, Proc. 24th EPS Conf. Contol. Fusion and Plasma Physics, **1**, 277 (1997).

[6] A. Thyagaraja, Plasma Phys. Control. Fusion **35**, 1037, (1994). The present paper summarizes in part the presentation made at the Fifth IAEA Technical Committee Meeting on Alpha Particles in Fusion Research, at JET, Abingdon, UK, Sept. 1997 by Thyagaraja *et al.*

[7] G. Vlad, C. Kar, F. Zonca and F. Romanelli, Phys. Plasmas, **2**,418 (1995).

[8] C.N. Lashmore-Davies, A. Thyagaraja and R.A. Cairns, Phys. Plasmas, **4**, 3243 (1997).

[9] H.L. Berk and B.N. Breizman, *Phys Fluids*, **B2**, 2246 (1990).

[10] Y.M. Li, S.M. Mahajan, and D.W. Ross, Phys. Fluids, **30**, 1466 (1987).

[11] A. Thyagaraja, C.N. Lashmore-Davies, R.A. Cairns, *The ideal MHD continuous spectrum in a cylindrical screw pinch: a question of completeness*, UKAEA Fusion report, UKAEA FUS385, (1998). To appear in Phys. Plasmas. (Also presented at the Atlanta Sherwood Meeting, Mar. 1998).

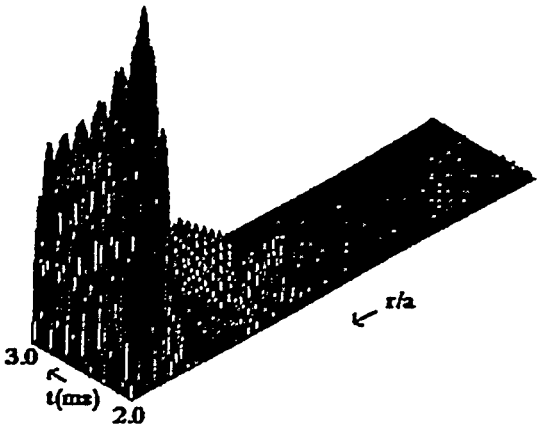

Figure 1 RMS Vorticity in nonlinearly saturated TAE

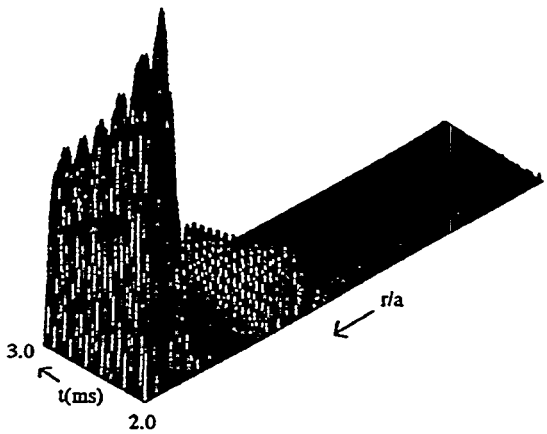

Figure 2 RMS Current in nonlinearly saturated TAE

Adaptive Mesh Refinement for Current Sheets

C. Marliani
Courant Institute of Mathematical Sciences
New York University

I. Introduction

The dynamics of current sheet formation and magnetic reconnection are studied in the framework of incompressible magnetohydrodynamics. Using Elsässer variables $\mathbf{z}^{\pm} = \mathbf{u} \pm \mathbf{B}$, the MHD equations take the symmetric form

$$\partial_t \mathbf{z}^{\pm} + \mathbf{z}^{\mp} \cdot \nabla \mathbf{z}^{\pm} = \mu_+ \Delta \mathbf{z}^{\pm} + \mu_- \Delta \mathbf{z}^{\mp} - \nabla p \,, \quad \nabla \cdot \mathbf{z}^{\pm} = 0$$

where $\mu_{\pm} = (\nu \pm \eta)/2$ and ν is the viscosity, η the resistivity and p the sum of ordinary and magnetic pressure.

In spite of their unphysical nature the singular structures of the inviscid, ideal equations, $\nu = \eta = 0$, are not only of mathematical interest. They provide an effective mechanism for transport of energy to small scales and as they determine the behavior of higher order structure functions they play an important role in current attempts towards understanding fully developed turbulence, e.g. [5]. Last but not least, for us the singular structures serve to put the adaptive numerics to a stringent test for in the dynamics of the non-dissipative equations lacking spatial resolution is easily detected.

II. Numerical method

There are a number of codes using adaptive unstructured mesh methods for magnetohydrodynamic flows but only very few based on structured meshes.

Our adaptive mesh scheme for incompressible fluid and plasma flows consists of two parts which are largely independent of each other, namely the integration scheme for each grid and the adaptive mesh refinement algorithm. Their independence makes it easy to exchange the equations to be studied.

The single-grid integration scheme is a projection method with second order upwinding which has already been used in former non-adaptive simulations [6]. The method is an adaption of work for the Navier–Stokes equations [1] to magnetohydrodynamics. In the current context it only is important to note that the upwind scheme is stable even in the presence of discontinuities and locally introduces considerable numerical dissipation where underresolved steep gradients occur.

Our strategy for adaptive mesh refinement was motivated by work on shock hydrodynamics [2]. Our algorithm [4] consists of two main parts of which one is the recursive integration of a given hierarchy of grids and the other one is the regridding part which builds the grid hierarchy and dynamically adjusts it to the requirements of the flow.

The integration of the grid hierarchy starts by advancing the coarsest level's grid by a timestep Δt. The single grid integration scheme calculates the new Elsässer fields and the vorticities $\omega^{\pm} = \omega \pm j$ with fluid vorticity ω and current j. The potentials $\psi^{\pm}$ are obtained by inversion

of Poisson's equation $\Delta\psi^{\pm} = \omega^{\pm}$. Now the next finer grids are integrated. Here, the spatial discretization length and the time step are reduced by the refinement factor r, i.e. on these grids r timesteps have to be performed before the coarser one will be advanced again. All this is done recursively on the whole hierarchy down to the finest level. To be able to use the standard integration scheme on each of the grids ghost cells are needed around the boundary. The necessary data are either provided by neighboring grids of the same level or have to be interpolated in space and time from the next coarser level. The vorticities being the highest order derivatives are linearly interpolated and the stream functions are obtained as the solution of Poisson's equation.

After a given number of timesteps it is checked whether the resolution is still sufficient on the whole integrational domain. Reasonable choices for the refinement criterion are either the local error based on the difference of the nonlinearity on a mesh with the actual and twice the discretization length or physically motivated criteria based on the absolute values of the vorticities or the maximum's norm of the gradient of the Elsässer fields. Independent of which criterion is chosen it is essential to guarantee convergence by varying the threshold for marking points. All marked points are appended to a list and in addition with each point some surrounding points are included. The size of this neighborhood is proportional to the number of timesteps until the next check for sufficient resolution will be done and the local velocity. The next step is the grid generation in order to find a list of rectangles which cover the marked points. It starts on one rectangle covering all and then recursively performs cuts. Evaluation of a function measuring the costs for integrating on the actual list of rectangles leads to some optimal covering. The rectangles are then filled with data either from already existing grids of the same or by interpolation from the next coarser level. Then it is checked whether this new level's resolution is sufficient. All this is done recursively.

Having in mind the recursive procedures and the various lists to be managed, it is obvious that using an object oriented language as C++ is the most appropriate choice. Nevertheless for the solution of Poisson's equation standard Fortran code is used for its speed.

III. Simulations

We studied the dynamics of the ideal MHD equations starting with some generic cases as a periodic box with Orszag–Tang or Biskamp–Welter initial conditions, the latter being made less symmetric by introducing arbitrary phase shifts [3]. In either case current sheets are forming and after a transitional phase the absolute maximum of current density is growing exponentially and the diameter of the sheet decreases exponentially in time. Figure 1 shows vorticity and current density at the end of the calculation in the Orszag–Tang case.

The simulations start on an initial grid with 256^2 mesh points and whenever the resolution becomes insufficient refinements are done. The resulting hierarchy of finer and finer grids dynamically adjusts to the flow and ensures sufficient resolution over the whole integrational domain. Whereas former simulations of the ideal equations [9] with classical integration schemes soon ran out of resolution, we can avoid any dissipation. Of course, as the current density continues to increase the simulations have to end at some point either due to the limited amount of memory available on the machine or because of becoming to expensive in computational time. In the present simulations typically up to 7 refinements by a factor two could be carried out leading to

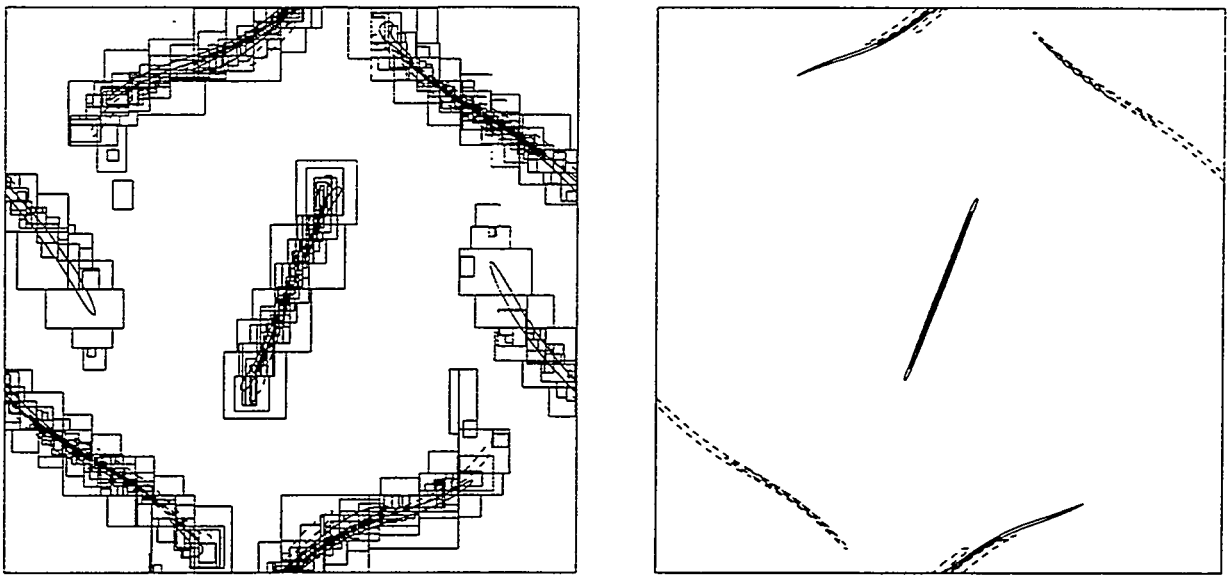

Figure 1: Contour plots of vorticity with grid hierarchy (left) and current density (right).

a final resolution that compares to 32768^2 grid points with non-adaptive treatment.

The ratio of the number of grid points in the adaptive simulations to that in comparable non-adaptive ones may serve as a measure of the efficiency of the code. In the case of ideal 2D MHD it is typically about 2%. The efficiency of an adaptive treatment is obviously related to the codimension of the structures to be resolved. In addition it increases with the number of refined levels.

Recently, we studied the coalescence instability for a checkerboard-like pattern of magnetic islands which is unstable towards a small perturbation leading to the formation of current sheets between two magnetic islands with the same sign. Note that for a symmetric initial perturbation in the kinetic stream function the positions of current sheets are known in advance thus allowing for simpler refinement methods to be successfully applied [8].

As in the previous examples the absolute value of current density is found to grow exponentially. Whereas in the ideal case the length of the sheets remains small during the entire simulation (with a final resolution corresponding to 32768^2 grid points on a non-adaptive mesh) they start to broaden if a small resistivity is included leading to pentagon-like patterns.

In the absence of any viscosity higher and higher resolution is needed to resolve the vorticity field which continues to grow exponentially. Therefore in the studies of reconnection we used a fixed value for viscosity. Simulations of merging islands have been carried out for different values of resistivity.

IV. Recent developments and outlook

The techniques used in two dimensions easily translate to higher dimensions. Therefore in the implementation of the adaptive mesh refinement part the spatial dimension becomes merely a

parameter. A code for the integration of the incompressible three-dimensional Euler equations was successfully applied in order to study singularity formation [7].

As already pointed out in the description of the numerical method the single-grid integration scheme and the adaptive mesh refinement algorithm are largely independent of each other. Thus implementing a three-dimensional MHD code was not a big effort. Studies of singularity formation and work on reconnection phenomena in the full 3D case are currently done.

Future work on treating complicated shaped boundaries in Cartesian grid methods will open an even wider range of applications. In addition it will enable us to investigate a lot of more applied problems in fluid and plasma flows.

References

[1] J. B. Bell, P. Colella, and H. M. Glaz. *J. Comput. Phys.*, 85:257–283, 1989.

[2] M. J. Berger and P. Colella. *J. Comput. Phys.*, 82:64–84, 1989.

[3] D. Biskamp and H. Welter. *Phys. Fluids B*, 1:1964–1979, 1989.

[4] H. Friedel, R. Grauer, and C. Marliani. *J. Comput. Phys.*, 134:190–198, 1997.

[5] R. Grauer, J. Krug, and C. Marliani. *Physics Lett. A*, 195:335–338, 1994.

[6] R. Grauer and C. Marliani. *Phys. Plasmas*, 2(1):41–47, 1995.

[7] R. Grauer, C. Marliani, and K. Germaschewski. Adaptive mesh refinement for singular solutions of the incompressible Euler equations. *submitted to Phys. Rev. Lett.*, 1997.

[8] D. W. Longcope and H. R. Strauss. *Phys. Fluids B*, 5(8):2858–2869, 1993.

[9] P. L. Sulem, U. Frisch, A. Pouquet, and M. Meneguzzi. *J. Plasma Phys.*, 33:191–198, 1985.